

PRESENT STATUS OF THE PHENOMENOLOGICAL REGGE POLE THEORY. I

BY

Masako BANDO and Katsusada MORITA

Department of Physics, Kyoto University, Kyoto

(Received October 1, 1968)

ABSTRACT

In this paper we present a systematic review of recent developments in phenomenological Regge pole theory of high energy scatterings.

CONTENTS

- §1. Introduction
- §2. Gross features of experimental data on angular distributions
 - 2.1 Coulomb interference region
 - 2.2 Forward diffraction region
 - 2.3 Structures at intermediate angles
 - 2.4 Backward region
- §3. Regge pole analysis of forward scatterings
 - 3.1 Single pole analysis and spin-flip phenomena
 - 3.1.1 $\pi^-p \rightarrow \pi^0n$
 - 3.1.2 $\pi^-p \rightarrow \eta n$
 - 3.1.3 Charge exchange quasi-two-body reactions
 - 3.2 Two-pole analysis
 - 3.2.1 $K^-p \rightarrow \bar{K}^0n$ and $K^+n \rightarrow K^0p$
 - 3.2.2 $p n \rightarrow n p$ and $\bar{p} p \rightarrow \bar{n} n$
 - 3.3 Many-pole analysis
 - 3.3.1 πN elastic scattering
 - 3.3.2 KN and $\bar{K}N$ elastic scatterings
 - 3.3.3 NN and $\bar{N}N$ elastic scatterings
- §4. Fermion Regge pole and backward meson-nucleon scattering
 - 4.1 Signature zero
 - 4.2 Gribov phenomenon
 - 4.3 $\pi^\pm p$ backward scattering
 - 4.4 $K^\pm p$ backward scattering
- §5. Polarization and possible non-Regge-pole effects
 - 5.1 Experimental results
 - 5.2 Pure Regge pole model
 - 5.3 Modified Regge pole model for π^-p charge exchange scattering
 - 5.3.1 $\rho + \rho'$ model
 - 5.3.2 $\rho +$ direct channel resonance model

5.3.3 $\rho+$ Regge cut model

5.3.4 $\rho+$ absorption model

§6. Resonance production and decay correlation

6.1 Density matrix and decay correlation

6.2 Regge pole analysis and possible modifications

§7. Concluding remarks

§1. Introduction

This is the first in a series of papers devoted to Regge phenomenology. In the last few years it has become widely accepted that the Regge pole expansion of the scattering amplitudes is a very useful tool in describing high energy scatterings. As yet we have no complete theory to state where Regge poles come from and to predict all their parameters. Experiments indicate some characteristic features that can be easily incorporated in the Regge pole model and comparison with Regge predictions has shed light on the properties of the residue and trajectory functions of the poles involved. The results, however, scatter in the literature and we feel it is necessary to review the whole situation.

The following properties of Regge poles are now familiar to us all:¹⁾

- a) Shrinkage of forward peak
- b) Phase-signature relation
- c) Asymptotic power-law behaviour of amplitude
- d) Factorization of residue
- e) Connection with particles and resonances
- f) Line-reversal²⁾

Brief elucidation on "line-reversal" should be necessary. Consider $\pi^\pm p$ elastic scattering. Contributors are Pomeranchon P , Igi pole P' and ρ . Let us write $\pi^\pm p$ amplitude in the form of

$$A(\pi^\pm p \rightarrow \pi^\pm p) = A_P + A_{P'} + A_\rho. \quad (1.1)$$

Then, changing the meson from π^+ to π^- (i. e., reversing the meson lines) which is equivalent to charge conjugation operation C in the crossed channel amounts to sign change in odd signature amplitude A_ρ :

$$A(\pi^- p \rightarrow \pi^- p) = A_P + A_{P'} - A_\rho \quad (1.1)'$$

This comes from the fact that $C=P=(-)^L=P_J$ for $\pi^+\pi^-$ rest system where P =ordinary parity, P_J =signature and L =orbital angular momentum. Another examples are given below.

$$\begin{aligned} A(K^+ p \rightarrow K^+ p) &= A_P + A_{P'} + A_\omega + A_\rho + A_R, \\ A(K^- p \rightarrow K^- p) &= A_P + A_{P'} - A_\omega - A_\rho + A_R, \\ A(K^+ n \rightarrow K^+ n) &= A_P + A_{P'} + A_\omega - A_\rho - A_R, \\ A(K^- n \rightarrow K^- n) &= A_P + A_{P'} - A_\omega + A_\rho - A_R. \end{aligned} \quad (1.2)$$

For reversing the spinor line, we must also charge conjugate the Dirac matrices connecting the initial and final Fermions belonging to reversed lines and new factors of +1 or -1 will appear in the coefficients of new invariant amplitudes. A special case of forward elastic scattering and no spin flip is very simple, the result being written in terms of total cross section through optical theorem:³⁾

$$\begin{aligned}
\sigma_T(p\bar{p}) &= \sigma_P + \sigma_{P'} + \sigma_\omega + \sigma_\rho + \sigma_R, \\
\sigma_T(pn) &= \sigma_P + \sigma_{P'} + \sigma_\omega - \sigma_\rho - \sigma_R, \\
\sigma_T(\bar{p}p) &= \sigma_P + \sigma_{P'} - \sigma_\omega - \sigma_\rho + \sigma_R, \\
\sigma_T(\bar{p}n) &= \sigma_P + \sigma_{P'} - \sigma_\omega + \sigma_\rho - \sigma_R.
\end{aligned}
\tag{1.3}$$

Here σ_p denotes Pomeron contribution to $\sigma_T(p\bar{p})$ and so on.

Since 1966 renewed attention has been drawn to the following characteristics of Regge poles some of which have already noticed by some authors in the early stage of Regge-pole theory:

- g) Nonsense and ghost-killing zeros^{4),5)}
- h) Signature zero⁶⁾
- i) Pairing of Fermion trajectory⁷⁾ and backward meson-nucleon scattering⁸⁾
- j) Conspiracy among Regge poles⁸⁾⁻¹⁰⁾

The zeros in Reggeized amplitude of types g) and h) are expected to develop dips in $d\sigma/dt$ if the pole in question has important contribution. The property i) is sometimes called Gribov phenomenon and associated with the MacDowell symmetry for partial-wave amplitude of π - N scattering.¹¹⁾ A remarkable property of "conspiracy" between Regge poles has already been realized by Volkov and Gribov⁸⁾ in 1962 and recent investigations by Freedman and Wang⁹⁾ and by Durand¹⁰⁾ reveals the existence of "daughter" trajectories which implies complicated situation in Regge-pole phenomenology.

As for spin dependence of scattering amplitude in a pure Regge pole model we have trouble with experiment. In particular, polarization in $\pi^-p \rightarrow \pi^0n$ and the (0, 0) component of ω meson density matrix in $\pi N \rightarrow \omega N$ (or Δ) should vanish because only ρ contributes, whereas experiments show finite polarization and nonvanishing ρ_{00} . Some background contributions must be taken into account but they are not unique.

Our main purpose here is to explain the close connection between the above-mentioned properties of Regge poles and the observed features of high energy elastic and elastic-like reactions. In order not to make the paper too lengthy the subject of conspiracy will be treated in a forthcoming paper.

§ 2. Gross features of experimental data on angular distributions

2. 1 Coulomb interference region ($|t| < 10^{-2}$ (GeV/c)²)

Table I. Ratio of real to imaginary parts of forward amplitude for elastic πN , KN and NN collisions.

Collision system	α	p_L in GeV/c
$p\bar{p}$	$-0.3^{12)}$	$p_L = 5 \sim 27$
pn	$-0.3^{13)}$	$p_L = 7 \sim 19$
$\bar{p}p$		
π^+p	-0.10 to $-0.07^{14)}$	$p_L = 10 \sim 14$
π^-p	-0.3 to $0.0^{14)}$	$p_L = 8 \sim 24$
K^+p	$0.31 \pm 0.21^{15)}$	$p_L = 3.5$
	0.45 ± 0.14	$p_L = 5.0$ sign undetermined
K^-p	$0.1 \pm 0.2^{16)}$	$p_L = 4.1$
	0.2 ± 0.2	$p_L = 5.5$ sign undetermined

Table I presents the ratio of real to imaginary parts of forward amplitudes for elastic πN , KN and NN collisions :

$$\alpha = \frac{Re A(s, 0)}{Im A(s, 0)} \quad (2.1)$$

For charge-exchange scatterings (see Table II), we compare, if possible, the differential cross sections at $t=0$ with the optical theorem value by which we mean :

Table II. Real over imaginary ratio for charge-exchange processes (O. T. V. = Optical Theorem Value)

processes	α	compared with optical value	structures at small angles
$\pi^- p \rightarrow \pi^0 n$	1 \pm 0.3	>O. T. V. ¹⁹⁾	forward dip ¹⁹⁾
$\pi^- p \rightarrow \eta n$			forward dip ²⁰⁾
$K^- p \rightarrow \bar{K}^0 n$		<O. T. V. ²¹⁾	forward dip ²¹⁾
$K^+ n \rightarrow K^0 p$		>O. T. V. ²²⁾	very sharp forward peak ²²⁾
$p n \rightarrow n p$		Not clear ²³⁾	
$\bar{p} p \rightarrow \bar{n} n$			

for $\pi^- p \rightarrow \pi^0 n$,

$$\frac{d\sigma}{dt}(\pi^- p \rightarrow \pi^0 n)_{opt.} = \frac{1}{16\pi} [\sigma_T(\pi^+ p) - \sigma_T(\pi^- p)]^2, \quad (2.2)$$

for $K^- p \rightarrow \bar{K}^0 n$,

$$\frac{d\sigma}{dt}(K^- p \rightarrow \bar{K}^0 n)_{opt.} = \frac{1}{16\pi} [\sigma_T(K^- p) - \sigma_T(K^- n)]^2, \quad (2.3)$$

for $K^+ n \rightarrow K^0 p$,

$$\frac{d\sigma}{dt}(K^+ n \rightarrow K^0 p)_{opt.} = \frac{1}{16\pi} [\sigma_T(K^+ p) - \sigma_T(K^+ n)]^2, \quad (2.4)$$

for $p n \rightarrow n p$,

$$\frac{d\sigma}{dt}(p n \rightarrow n p)_{opt.} = \frac{1}{16\pi} [\sigma_T(p p) - \sigma_T(p n)]^2, \quad (2.5)$$

and

for $\bar{p} p \rightarrow \bar{n} n$,

$$\frac{d\sigma}{dt}(\bar{p} p \rightarrow \bar{n} n)_{opt.} = \frac{1}{16\pi} [\sigma_T(\bar{p} p) - \sigma_T(\bar{p} n)]^2. \quad (2.6)$$

2. 2 Forward diffraction region ($|t| < 0.5(\text{GeV}/c)^2$)

As is well known the diffraction peak observed experimentally is well described by the formula

$$\frac{d\sigma}{dt} = \frac{d\sigma}{dt} \Big|_{t=0} e^{\gamma t} \quad (2.7)$$

where γ depends weakly on the energy. In Table III, the values of γ are given for various elastic and charge exchange scatterings (S denotes "shrinks", E "expands" and C "constant").

Table III. Slope of diffraction peak for elastic and charge-exchange scatterings and its energy dependence.

Collision system	γ in $(\text{GeV}/c)^{-2}$	Be- haviour	p_L in GeV/c	n from $(d\alpha/dt)_{t=0} \propto p_L^{-n}$
$p p$	7 to $10^{12,17)}$	S	$p_L=5\sim 27$	
$p n$	7 to $10^{18)}$	S	$p_L=2\sim 7$	
$\bar{p} p$	12 to $9^{17)}$	E	$p_L=12\sim 16$	
$\pi^+ p$	$9^{17)}$	C	$p_L=10\sim 14$	
$\pi^- p$	$9^{17)}$	C	$p_L=8\sim 24$	
$K^+ p$	4 to $7^{15,17)}$	S	$p_L=3.5\sim 5$	
$K^- p$	$9^{16,17)}$	C	$p_L=4.1\sim 5.5$	
$\pi^- p \rightarrow \pi^0 n$	$11^{19)}$	S	$p_L=3.07\sim 18.0$	1.3 ± 0.2
$\pi^- p \rightarrow \eta n$	$4\sim 5^{20)}$	S	$p_L=2.9\sim 18.2$	1.5 ± 0.1
$K^- p \rightarrow \bar{K}^0 n$	$5^{21)}$	S	$p_L=2\sim 9.5$	1.5 ± 0.2
$K^+ n \rightarrow K^0 n$				
$p n \rightarrow n p$	50 for $ t < 0.02^{22)}$ 5 for larger $ t $	S	$p_L=2\sim 8$	3.0
$\bar{p} p \rightarrow \bar{n} n$	$4.5^{23)}$	C	$p_L=5\sim 9$	1.7 ± 0.3
$\bar{p} p \rightarrow \bar{\Lambda} \Lambda$	Sharp forward peak ²⁴⁾		$p_L=3.0\sim 6.94$	1.9 ± 0.3

 2.3 Structures at intermediate angles ($0.5 < |t| < 1.5$)

Table IV. Structures at intermediate angles.

Collision system	Structures
$p p$	No. ²⁵⁾
$p n$	Shoulder at $t \approx -1$ $(\text{GeV}/c)^2$ ¹⁸⁾
$\bar{p} p$	dip at $t \approx -0.45$ ($1 < p_L < 2.5$) ²⁶⁾ (also at $p_L = 3.66$) ²⁷⁾ bump at $t \approx -0.8$ ($1 < p_L < 2.5$) Structure seems to vanish rapidly with increasing energy.
$\pi^+ p$	dip at $t \approx -0.7$ ($2 < p_L < 4$) ²⁸⁾ bump at $t \approx -1.2$ ($2 < p_L < 4$) Structure disappears quickly as energy increases.
$\pi^- p$	as for $\pi^+ p$ ²⁸⁾
$\pi^- p \rightarrow \pi^0 n$	dip at $t \approx -0.6$ ¹⁹⁾ bump at $t \approx -1$
$\pi^- p \rightarrow \eta n$	no dip ²⁰⁾
$K^- p \rightarrow \bar{K}^0 n$	probably no dip ²¹⁾
$p n \rightarrow n p$	No. ²²⁾
$\bar{p} p \rightarrow \bar{n} n$	No. ²³⁾

 2.4 Backward region $(-1 (\text{GeV}/c)^2 \geq u \geq -\frac{(M_N^2 - m_\pi^2)^2}{s})$

The observed backward peak for $\pi^\pm p$ scattering is consistent with the formula

$$\frac{d\sigma}{du} = \frac{d\sigma}{du} \Big|_{\theta=180^\circ} \cdot e^{\gamma(u-u_{max})} \quad (2.8)$$

where γ depends rather strongly on energy as shown in Table V.

Table V. Meson-Nucleon scattering in the backward hemisphere.

particle system	γ in $(\text{GeV}/c)^{-2}$	Structure
$\pi^+p \rightarrow p\pi^+$	$12 \leq \gamma \leq 20$ at $p_L = 4^{(29), (30)}$ $13 \leq \gamma \leq 27$ at $p_L = 8$	dip at $u \approx 0.2$ $(\text{GeV}/c)^2$
$\pi^-p \rightarrow p\pi^-$	$3.8 \leq \gamma \leq 10$ at $p_L = 4$ (1/5 of π^+p) $10 \leq \gamma \leq 15$ at $p_L = 8$	no dip backward dip ³¹⁾
$K^+p \rightarrow pK^+$	Small indication of backward scattering at $p_L = 3.5, 5.0^{(31), (32)}$	
$K^-p \rightarrow pK^-$	No indication of backward scattering at $p_L = 4.1, 5.5^{(32)}$	

§ 3. Regge pole analysis of forward scatterings

Let us recapitulate briefly the basic formula of Regge pole theory for relativistic scattering.¹⁾ Consider a scattering of two spinless, equal-mass particles. In the t -channel center of mass system the usual invariant variables are

$$\begin{aligned} t &= 4(p_i^2 + m^2) \\ s &= -2p_i^2(1 + \cos\theta_i) \\ u &= -2p_i^2(1 - \cos\theta_i) \end{aligned}$$

where p_i and θ_i are the magnitude of relative momentum and the scattering angle. Denote the t -channel scattering amplitude by $f^t(t, z_i)$ and expand it into partial-waves :

$$f^t(t, z_i) = \sum_{j=0}^{\infty} (2j+1) f_j^t(t) P_j(z_i) \quad (z_i = \cos\theta_i) \quad (3.1)$$

Assuming for f^t a fixed- t dispersion relation with N subtractions and using the inverse formula of (3.1), we can perform the Froissart-Gribov continuation of f_j^t (call it $f^{\pm}(t, J)$, \pm designates signature) for $\text{Re}J < N$ where $f^{\pm}(t, J)$ turns out to be holomorphic. For Carlson's theorem to hold in the presence of exchange forces, the continuation has to be made separately away from even and odd J values whence we meet the concept of signature. Let us further assume the analytic continuation for $\text{Re}J < N$ of $f^{\pm}(t, J)$ has no singularities other than Regge poles at $J = \alpha_i^{\pm}(t)$. Transforming (3.1) by the method of Sommerfeld and Watson and picking up Regge poles, one finds

$$\begin{aligned} f^t(t, z_i) &= -\pi \sum_i \frac{(2\alpha_i^+ + 1) b_i^+(t)}{\sin\pi\alpha_i^+} \left\{ \frac{P_{\alpha_i^+}^+(-z_i) + P_{\alpha_i^+}^+(z_i)}{2} \right\} \\ &\quad - \pi \sum_i \frac{(2\alpha_i^- + 1) b_i^-(t)}{\sin\pi\alpha_i^-} \left\{ \frac{P_{\alpha_i^-}^+(-z_i) - P_{\alpha_i^-}^+(z_i)}{2} \right\} \\ &\quad + \text{background integral,} \end{aligned} \quad (3.2)$$

where $b_i^{\pm}(t)$ is residue of pole at $J = \alpha_i^{\pm}(t)$. Using crossing symmetry, the asymptotic form of eq. (3.2) for large z_i (or s) gives Regge pole contributions to high energy s -channel amplitude :

$$\begin{aligned} f^s(s, t) &\xrightarrow{s \rightarrow \infty} -\sqrt{\pi} \sum_i \frac{\gamma_i^+(t) \Gamma\left(\alpha_i^+ + \frac{3}{2}\right)}{\Gamma(\alpha_i^+ + 1)} \xi_i^+(t) \left(\frac{s}{s_0}\right)^{\alpha_i^+(t)} \\ &\quad - \sqrt{\pi} \sum_i \frac{\gamma_i^-(t) \Gamma\left(\alpha_i^- + \frac{3}{2}\right)}{\Gamma(\alpha_i^- + 1)} \xi_i^-(t) \left(\frac{s}{s_0}\right)^{\alpha_i^-(t)}, \end{aligned} \quad (3.3)$$

where

$$\xi_i^\pm(t) = \frac{1 \pm e^{-i\pi\alpha_i^\pm(t)}}{2\sin\pi\alpha_i^\pm(t)}, \quad (3.4)$$

and $r_i^\pm(t)$ is the reduced residue factored out the threshold behaviour $(2p_i^2)^{\alpha_i^\pm(t)}$ from $b_i^\pm(t)$ and s_0 is a scaling factor with dimension of squared energy.

For scattering of particles with spins³³⁾ the formula become complicated and new problems arise such as nonsense zero at $J=0$ and fixed singularities at the nonsense values of J of wrong signature. In the following we shall meet these frequently.

This and the subsequent sections will be devoted to discuss how the details of Regge trajectories have been unravelled through the analysis of experimental data in terms of them.

3. 1 Single-pole analysis and spin-flip phenomena

3. 1. 1 $\pi^-p \rightarrow \pi^0n$

Only ρ contributes to $\pi^-p \rightarrow \pi^0n$ ³⁴⁾⁻³⁸⁾, and the experiments¹²⁾ on this reaction

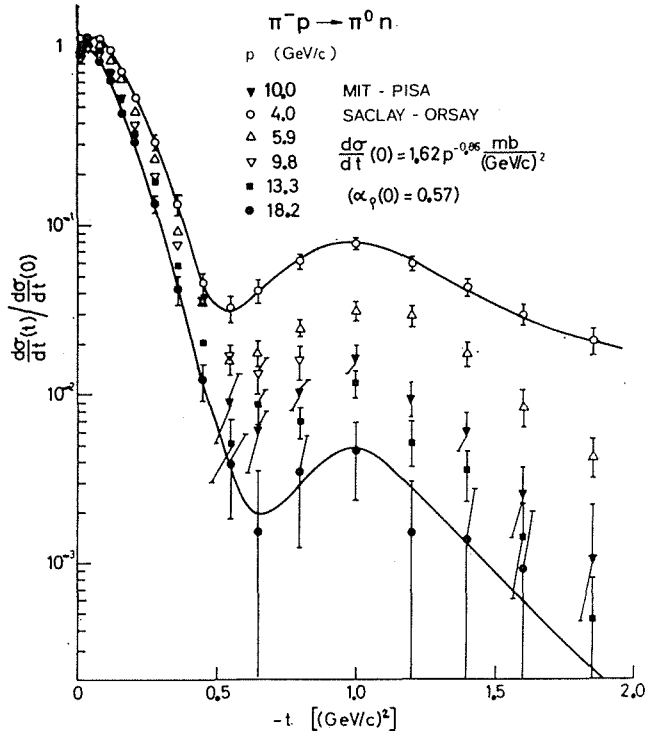


Fig. 3-1. The π^-p charge exchange differential cross section at various laboratory-system momenta. The data are from Ref. 19, I. Manneli et al., (MIT-PISA group) (\blacktriangledown 10.0 GeV/c); Ref. 19, A. V. Stirling et al. (SACLAY-ORSAY group) (\triangle 5.9, ∇ 9.8, \blacksquare 13.3, \bullet 18.2); Ref. 19, P. Sonderegger et al. (SACLAY-ORSAY) (\circ 4.0)

have confirmed the striking, qualitative features of a single-Regge-pole model :

- (1) Forward peak shrinks with increasing energy.
- (2) Re/Im ratio at $t=0$ is about 1. Remember that, since ρ has odd signature and its zero-intercept is about $1/2$, one has

$$\xi_\rho(t=0) = \frac{1 - e^{-i\pi\alpha_\rho(0)}}{2\sin\pi\alpha_\rho(0)} \approx \frac{1}{2}(1+i) \left(\alpha_\rho(0) \approx \frac{1}{2} \right) \quad (3.5)$$

or, in other words,

$$\frac{d\sigma}{dt}(\pi^-p \rightarrow \pi^0n) \text{ at } t=0 \approx 2 \text{ times O. T. V.}$$

(O. T. V. = optical theorem value)

- (3) Energy dependence at $t=0$ is

$$\frac{d\sigma}{dt} \text{ at } t=0 \propto s^{2\alpha_\rho(0)-2} \propto p_L^{-1}$$

(p_L = lab. mom. of pion)

which is also consistent with experiment (see Table III). However measured finite polarization³⁹⁾ of recoil neutron indicates some background contributions⁴⁰⁾ beyond ρ exchange :

- (4) Helicity-flip and -nonflip amplitudes are in phase when only one Boson trajectory is exchanged so that polarization must vanish.

The trajectory function is determined to be³⁵⁾

$$\alpha_\rho(t) = 0.58 + 1.02t \quad (3.6)$$

which is plotted in Fig. 1 along with R trajectory discussed below.

Now the angular distribution of differential cross section (see Fig. 3-1)

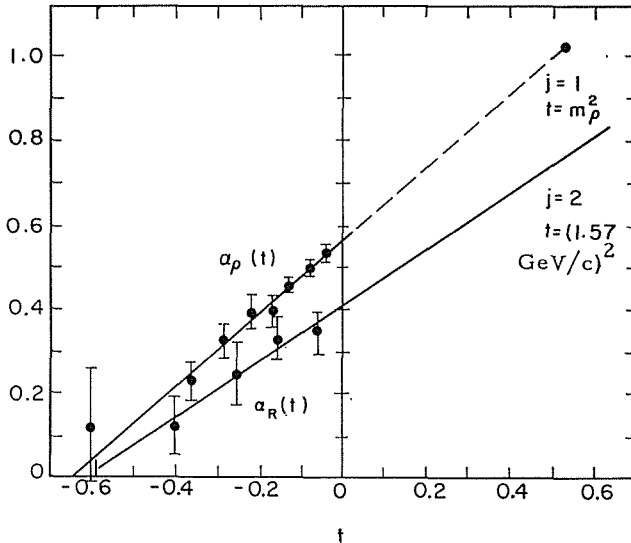


Fig. 1. The ρ and R trajectories as determined by Ter-Martirosyan (Ref. 46) using a Regge pole fit to $\pi^-p \rightarrow \pi^0n$ and $\pi^-p \rightarrow \eta n$ experimental data.

shows some remarkable structures; a forward dip at $t=0$ with subsequent turn-over near $t=-0.02$ (GeV/c)² and a second dip at $t \approx -0.6$ (GeV/c)² accompanying falling-off maximum near $t=-1.0$ (GeV/c)². These structures are commonly associated with the property that ρ couples strongly to helicity-flip amplitude. Crossed channel ($\pi^- \pi^0 \rightarrow \bar{p} n$) helicity-flip amplitude has a kinematically required factor $\sqrt{-t} \cdot \alpha_\rho(t)$ which induces zeros at $t=0$ and $t=t_a$ for which $\alpha_\rho(t_a)=0$. If helicity-flip amplitude is much larger than nonflip one, these zeros are expected to develop dips in $d\sigma/dt$ at respective t -values. Near $t=-0.6$ (GeV/c)² ρ seems to pass through spin zero (Fig. 1) ("nonsense transition of wrong signature").⁴¹⁾

3. 1. 2 $\pi^- p \rightarrow \eta n$

In this case only R can be exchanged in the crossed channel⁴²⁾⁻⁴⁶⁾ (R is assumed to be associated with A_2 meson having $J^{PG}=2^{+-}$, $I=1$ and mass 1320 MeV). This process also exhibits the striking features of one-pole model as in 3.1.1: the energy dependence at $t=0$ and the shrinking forward peak²⁰⁾. We have no data on polarization $P(\theta)$ for this process. R trajectory is given the Pignotti form⁴⁵⁾

$$\alpha_R(t) = -1 + \frac{1.35}{1 - 0.34t} \quad (3.7)$$

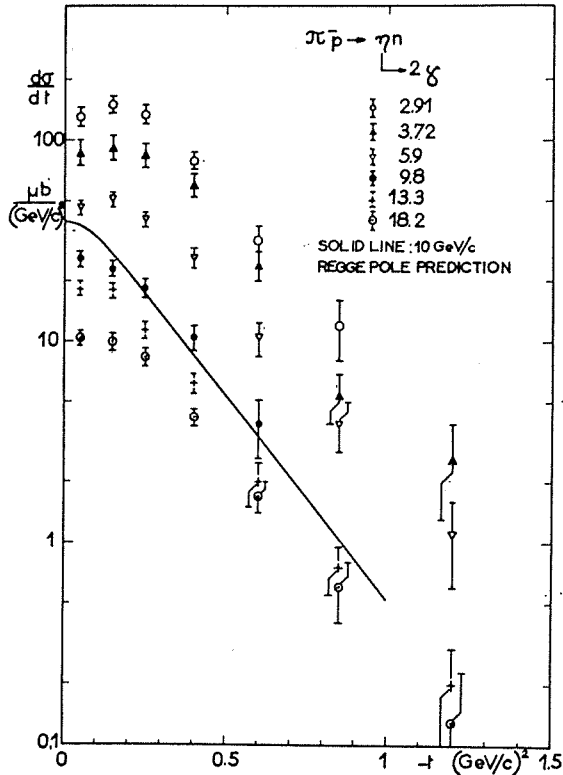


Fig. 3-2. Differential cross sections for the reaction $\pi^- p \rightarrow \eta n (\eta \rightarrow 2\gamma)$. Ref. 20 (SACLAY-ORSAY group). The solid line is the Regge pole prediction at 10 GeV/c from Ref. 44.

Linear trajectory plotted in Fig. 1 is determined by Ter-Martirosyan⁴⁶⁾.

Observed forward dip in $d\sigma/dt$ indicates strong coupling of R trajectory to helicity-flip amplitude. No indication of secondary dip near $t=-0.6$ (GeV/c)² seems to support Gell-Mann's mechanism⁴⁾ for avoiding $J=0$ ghost states which would otherwise occur for even signature trajectories. Another mechanism proposed by Chew⁵⁾ for removing such ghosts introduces an extra factor $\alpha_R(t)$ in the residue function which predicts a definite minimum in $d\sigma/dt$ when R passes through spin zero.⁴⁷⁾ Whether trajectories in even signature nonet chooses "nonsense" (Gell-Mann's type) or "sense" (Chew's type) at $J=0$ is an open theoretical question and is relevant also for $\pi^\pm p$ and $\bar{p}p$ elastic scatterings where, at energies up to about 3 GeV/c, dips near $t=-0.5$ (GeV/c)² have been observed.^{26)–29)}

In passing we remark that kinematical constraint due to the mass difference between π and η pointed out by Wang⁴⁸⁾ gives no significant effects.⁴⁵⁾

3. 1. 3 Charge exchange quasi-two-body reactions

We list below several quasi-two body processes in which only ρ or only R can be exchanged as in the above examples. These reactions are expected to exhibit some characteristics of one-pole exchange mechanism mentioned above. If experimental data are accumulated and show striking departures from single-pole prediction, then we must modify the single-pole approach by introducing low-ranking trajectories, direct channel resonances, Regge cut and so on.

Only ρ exchange :

$$\begin{aligned} \text{Charge exchange } \pi p &\longrightarrow \pi \Delta^{(49)-55), 57)} \\ \text{Charge exchange } \pi p &\longrightarrow A_{1,2} N \text{ (or } \Delta) \\ \pi p &\longrightarrow \omega n \text{ (or } \Delta)^{53) 56)} \end{aligned}$$

Note that ω production may involve B meson⁵⁸⁾ exchange.⁵⁹⁾

Only R exchange :

$$\pi N \longrightarrow \eta N \text{ (or } \Delta)^{53)}$$

3. 2 Two-pole analysis

3. 2. 1 $K^- p \longrightarrow \bar{K}^0 n$ and $K^+ n \longrightarrow K^0 p$

From Eq. (1.2) amplitudes for these processes are easily found, by using charge independence, to be

$$\begin{aligned} A(K^- p \longrightarrow \bar{K}^0 n) &= 2(-A_\rho + A_R) \\ A(K^+ n \longrightarrow K^0 p) &= 2(A_\rho + A_R) \end{aligned} \quad (3.8)$$

Since experimentally $\sigma_T(K^+ p) = \sigma_T(K^+ n)^{60)}$ within a few percent in the energy range $p_L = 6 \sim 20$ GeV/c, ρ and R residues in Eq. (3.8) should have the same sign at $t=0$ so that imaginary parts tend to cancel in $K^+ n \rightarrow K^0 p$, to wit,

$$\text{Im}A(K^+ n \longrightarrow K^0 p) \text{ at } t=0 \approx 0. \quad (3.9)$$

This predicts that

$$\begin{aligned} \frac{d\sigma}{dt}(K^- p \longrightarrow \bar{K}^0 n) \text{ at } t=0 &\approx \text{O. T. V.} \\ \frac{d\sigma}{dt}(K^+ n \longrightarrow K^0 p) \text{ at } t=0 &\gg \text{O. T. V.} \end{aligned} \quad (3.10)$$

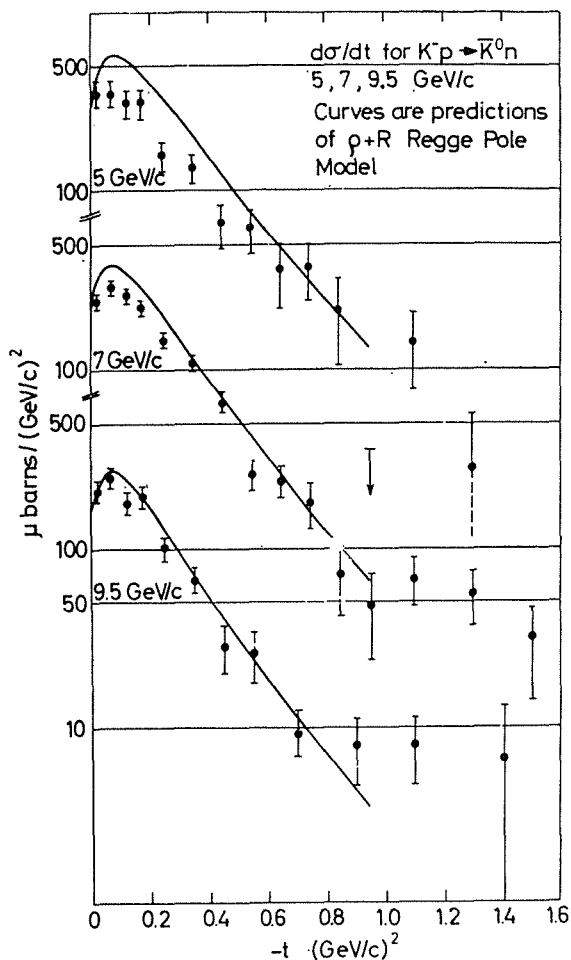


Fig. 3-3. The differential cross section for the reaction $K^-p \rightarrow \bar{K}^0n$ at laboratory-system momenta of 5, 7, and 9.5 GeV/c reported by Astbury et al. (CERN-ETH group) (Ref. 21). The theoretical curves are for a Regge pole model fit by Phillips and Rarita (Ref. 42). In this fit only the 9.5 GeV/c data were used and therefore the 5 and 7 GeV/c theoretical curves are predictions according to the model.

The former is consistent with experiment²¹⁾ (see Table II) but we have no high energy data on $K^+n \rightarrow K^0p$.

Since ρ and R have nearly equal zero-intercept (about $1/2$), one predicts (see Table III)

$$\frac{d\sigma}{dt} \text{ at } t=0 \propto p_L^{-1-1.5} \text{ for both reactions.}$$

Strong coupling of helicity-flip amplitude to both ρ and R as suggested from $\pi^-p \rightarrow \pi^0n$ and $\pi^-p \rightarrow \eta n$ can also explain the observed forward dip-turn-over sequence²⁸⁾ in $d\sigma/dt$ for $K^-p \rightarrow \bar{K}^0n$. However if helicity-flip ρ and R amplitudes

interfere destructively, such a dip-turn-over sequence should not appear. According to Phillips and Rarita,³⁵⁾ such a case happens for $K^+n \rightarrow K^0p$; this has to be checked experimentally.

On the other hand, there is no significant evidence for the presence of secondary dip in $K^-p \rightarrow \bar{K}^0n$ scattering for $p_L \geq 5$ GeV/c, indicating nonvanishing contribution of helicity-flip amplitude when ρ and R pass through spin zero (both near $t = -0.6$ (GeV/c)²). This must be due to R ("nonsense transition of right signature")⁶¹⁾ since ρ cannot spin-flip there.

Finally it is hoped that polarization parameters for these reactions will be measured by using polarized target in a near future in order to test this model further. From Eq. (3.8) one sees that $P(K^-p \rightarrow \bar{K}^0n) = -P(K^+n \rightarrow K^0p)$ for small momentum transfers.

3. 2. 2 $pn \rightarrow np$ and $\bar{p}p \rightarrow \bar{n}n$

In terms of $\rho+R$ model, we may write helicity amplitudes for these reactions as follows.

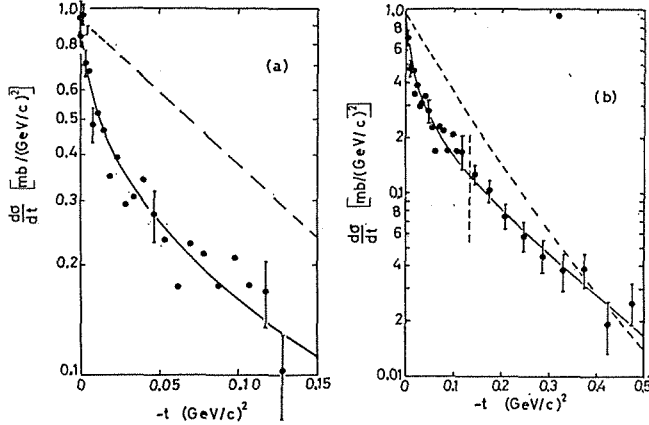


Fig. 3-4. Differential cross section for proton-neutron charge exchange at 8 GeV/c (Manning et al., Ref. 22); (a) covers laboratory angles 0 to 45 mrad; (b) 0 to 9 mrad. The broken line shows the results for p - p elastic cross section at 8.9 GeV/c (Foley et al., Ref. 17).

$$\begin{aligned}\phi_i(pn \rightarrow np) &= \phi_i^\rho + \phi_i^R, \\ \phi_i(\bar{p}p \rightarrow \bar{n}n) &= -\phi_i^\rho + \phi_i^R,\end{aligned}\quad (3.11)$$

where i runs from 1 to 5, corresponding to $++ \rightarrow ++$, $-- \rightarrow ++$, $+ - \rightarrow + -$, $- + \rightarrow + -$ and $+ - \rightarrow ++$ transitions in the center of mass system (\pm stands for helicities $\pm 1/2$) and the normalization is such that

$$\frac{d\sigma}{dt} = \frac{\pi}{2k^2} \{ |\phi_1|^2 + |\phi_2|^2 + |\phi_3|^2 + |\phi_4|^2 + 4|\phi_5|^2 \}, \quad (3.12)$$

and

$$\sigma_r = \frac{2\pi}{k} \text{Im} \{ \phi_1(t=0) + \phi_3(t=0) \} \quad (k = \text{c.m. momentum}) \quad (3.13)$$

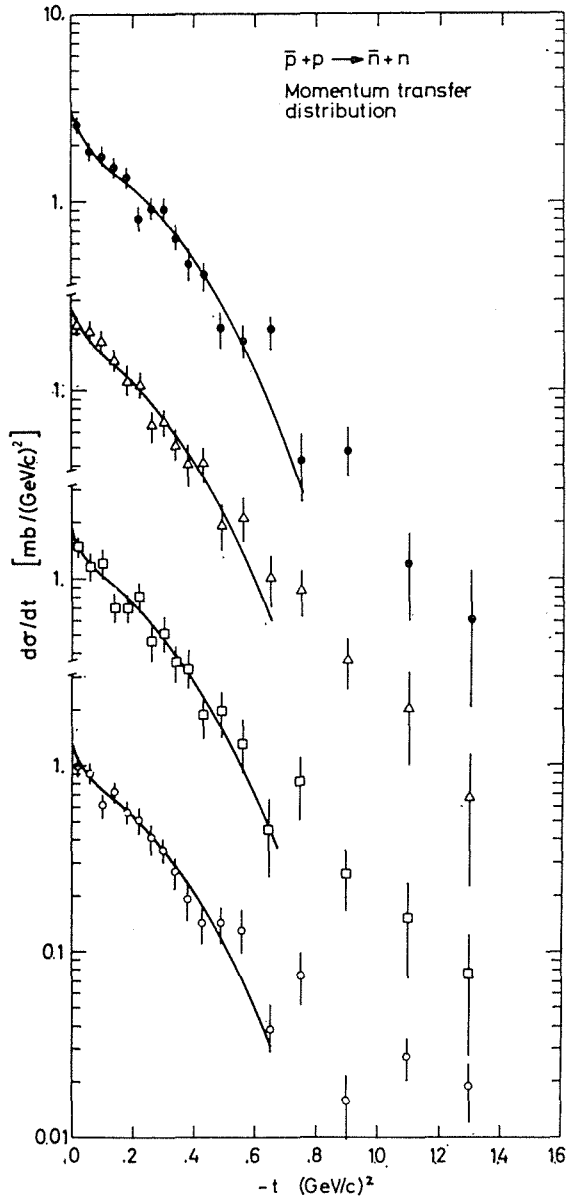


Fig. 3-5. The differential cross section for the reaction $\bar{p}p \rightarrow \bar{n}n$ for the momenta 5, 6, 7, and 9 GeV/c as measured by Astbury et al., Ref. 23. The theoretical predictions are for the coherent-droplet model. p_L (in GeV/c); ● 5; △ 6; □ 7; ○ 9.

Since experimentally $\sigma_r(p\bar{p}) - \sigma_r(pn) < \sigma_r(\bar{p}p) - \sigma_r(\bar{p}n)$ (for example, at $p_L=12$ GeV/c, LHS = -0.5 mb and RHS = 1.5 mb),⁶⁰⁾ we require that imaginary parts tend to cancel in $p\bar{n} \rightarrow n\bar{p}$, thus predicting

$$\begin{aligned} \frac{d\sigma}{dt}(p\bar{n} \rightarrow n\bar{p}) \text{ at } t=0 &> \text{O. T. V.} \\ \frac{d\sigma}{dt}(p\bar{p} \rightarrow n\bar{n}) \text{ at } t=0 &\approx \text{O. T. V.} \end{aligned}$$

See Table. II. Moreover we have

$$\frac{d\sigma}{dt} \text{ at } t=0 \propto p_L^{-1 \sim -1.5} \text{ for both reactions,}$$

as in KN charge exchange, while experiment shows more rapid decrease like $p_L^{-(2 \sim 3)}$ (Table III). Also as in KN charge exchange, a forward dip is expected at least for $\bar{p}p \rightarrow \bar{n}n$ but experiment indicates nothing.

Therefore we conclude that $\rho+R$ model cannot explain the energy dependence at $t=0$, the absence of forward dip and a sharp forward peak ($\sim \exp(-50t)$ for $|t| < 0.02$ (GeV/c)²) of $p\bar{n} \rightarrow n\bar{p}$.²²⁾ At this stage we note that trajectories belonging to pseudoscalar and axial vector nonets can couple to nucleons but not to pseudoscalar mesons so that they may play any role in NN and $\bar{N}N$ scatterings even though they are low-ranking. This will be studied in the second paper.

3. 3 Many-pole analysis

3. 3. 1 πN elastic scattering

Amplitudes for this case was given in Eq. (1. 1).

Non-shrinkage of forward peak could be supported by interference of P' and ρ with flatter trajectory p (its slope $\sim 1/3$ (GeV/c)⁻² or smaller). If P is flat, no observed particles lie on it and a logical question arises: What about the previous triumph concerning the f^0 meson? (C. N. Yang)⁶²⁾ Although there are some speculations, we shall not concern this point here but would not be surprised if there are complicated singularities like fixed poles or cuts in the complex angular momentum plane.⁴¹⁾

There is an interesting phenomenon, the so-called cross-over effect, in $\pi^\pm p$ differential cross sections which has been observed at each energy for $t \approx -0.05$ (GeV/c)². Phillips and Rarita³⁵⁾ suggested that this could be associated with either sign change of helicity-nonflip ρ amplitude at indicated t -value or opposite sign of interference terms between $P+P'$ and ρ for helicity-flip and -nonflip parts. The latter alternative does not introduce any zero in residues but the former does. This is also of importance in theoretical investigation on residue function.

At energies up to about 3 GeV/c, a dip has been observed near $t = -0.5$ (GeV/c)². Neglecting resonance effects in this angular region, Frautschi³⁷⁾ proposes that also P' cannot spinflip when it verifies $\alpha_{P'}(t) = 0$ just as in the case of ρ and that, since both ρ and P' seem to pass through spin zero at $t \approx -0.6$ (GeV/c)², the dip could be associated with the helicity-flip phenomena as in charge exchange. As it seems plausible to assume that P' and R belong to the same tensor nonet, R should bear the same property, which cannot be accepted

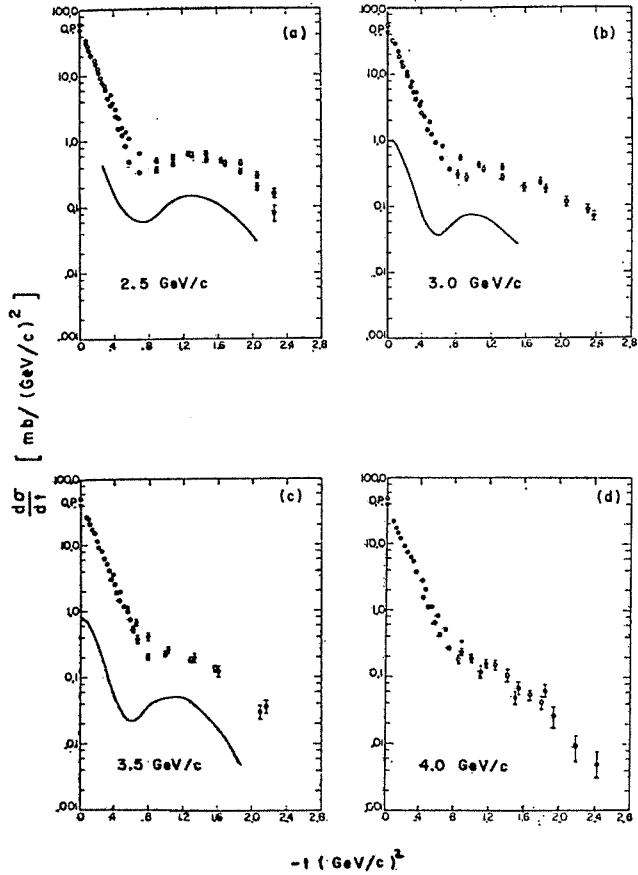


Fig. 3-6. Comparison of π^+p and π^-p elastic scattering differential cross sections at laboratory-system momenta of 2.5, 3.0, 3.5, and 4.0 GeV/c by Coffin et al. (Ref. 28). Also shown is a free hand fit to the π^-p charge exchange in the same momentum region.

$\pi^+p \rightarrow \pi^+p$, Michigan group (Ref. 28)

$\pi^-p \rightarrow \pi^-p$, Michigan group (Ref. 28)

Solid curve, $\pi^-p \rightarrow \pi^0n$:

(a) Carroll et al. 2.46 GeV/c

(b) Sonderegger et al. (Ref. 19), 3.07 GeV

(c) Sonderegger et al. (Ref. 19), 3.67 GeV

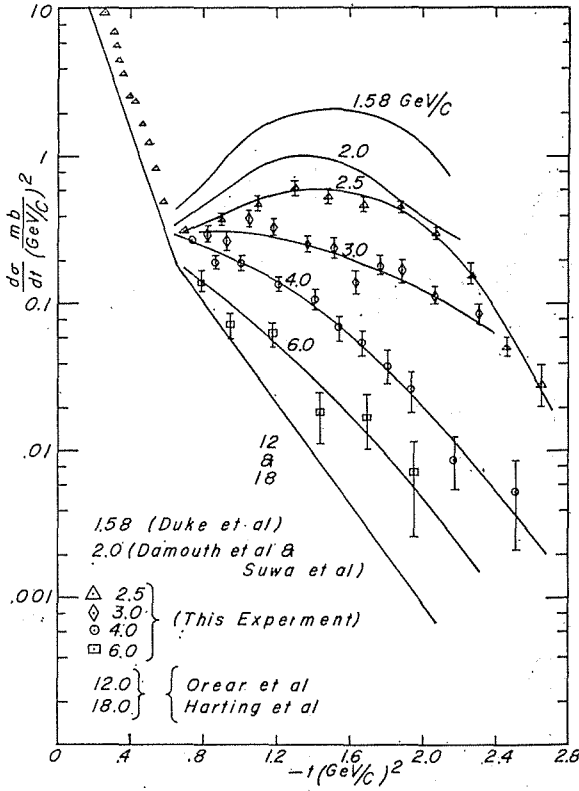


Fig. 3-7. Momentum dependence of π^+p elastic differential cross section. "This experiment" refers to the data by the Michigan group (Ref. 28). Refs: P. J. Duke et al., Phys. Rev. Letters 15, 468 (1965); D. E. Damouth et al., Phys. Rev. Letters 11, 287 (1963); S. Suwa et al., Phys. Rev. Letters 15, 560 (1965); D. Harting et al., Nuovo Cim. 38, 60 (1965).

from the discussion in 3.1.2. Whether trajectories in the even signature nonet give vanishing or finite helicity-flip when they verify $\alpha(t)=0$ should be further investigated both from experimental and theoretical point of views.⁶³⁾

Recent measurements on polarization parameters⁷⁰⁾ for $\pi^\pm p$ scattering provide an interesting test for Regge-pole description which will be considered in §5.

3. 3. 2 $\bar{K}N$ and $\bar{K}N$ elastic scatterings

As is indicated in Eq. (1.2) these contain five poles so that too many parameters are introduced in analyzing the data in terms of them. We shall not discuss these processes but only refer the reader to the paper by Phillips and Rarita.³⁵⁾

3. 3. 3 NN and $\bar{N}N$ elastic scatterings⁶⁴⁾

In this case contributors to total cross sections are five poles (Eq. (1.3)) but also trajectories belonging to pseudoscalar and axial-vector nonets contribute

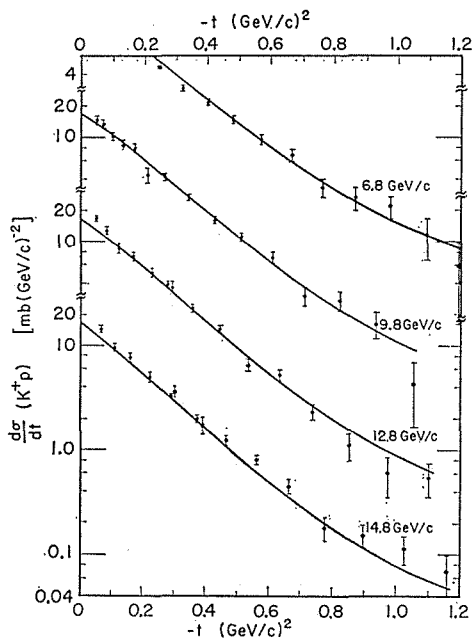


Fig. 3-8. K^+p differential cross section at 6.8, 9.8, 12.8 and 14.8 GeV/c from Ref. 17, compared with solution 1 of Phillips and Rarita (Ref. 35). Successive sets are spaced by a decade.

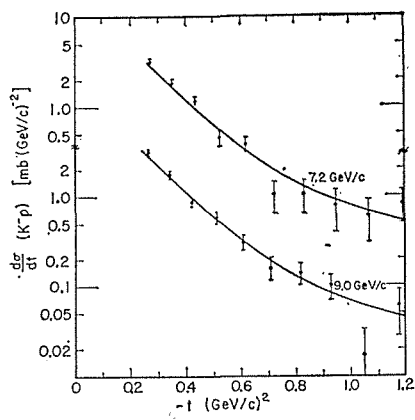


Fig. 3-9. K^-p differential cross sections at 7.2 and 9.0 GeV/c from Ref. 17, compared with solution 1 of Phillips and Rarita (Ref. 35). The two sets are spaced by a decade.

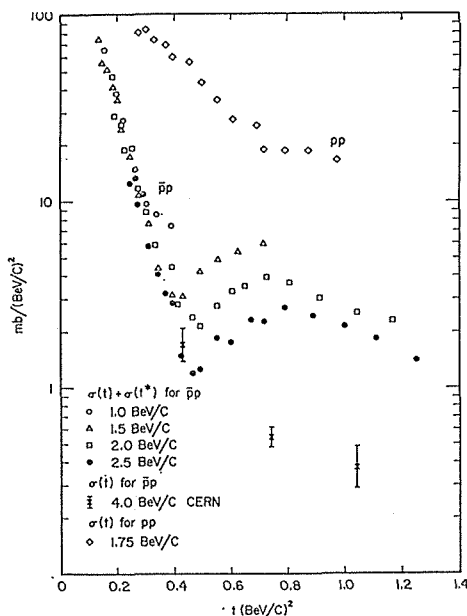


Fig. 3-10. $p-p$ elastic scattering distribution according to Barish et al. (Ref. 26); also shown for comparison is a $\bar{p}p$ distribution at 1.75 GeV/c. The $\bar{p}p$ points at 4.0 GeV/c are from Czyzewski et al., quoted by A. Whetherell in B.

to $d\sigma/dt$, $P(\theta)$ and so on and the situation becomes complicated if we further take into account the conspiracy among helicity amplitudes at $t=0$. This will be considered in a forthcoming paper.

§ 4. Fermion Regge pole and backward meson-nucleon scattering

This section will be further divided into three parts: the first deals with the signature zero (for simplicity, in the case of Boson trajectory), the second some peculiar properties of Fermion Regge pole and finally we shall study $\pi^\pm p$ backward scattering in terms of Fermion Regge pole exchange model.

4. 1 Signature zero

Let us turn back to Eq. (3.3) which we may rewrite as follows:

$$f^s(s, t) \xrightarrow{s \rightarrow \infty} -\sqrt{\pi} \sum_i \frac{\Gamma\left(\alpha_i^\pm + \frac{3}{2}\right) r_i^\pm(t)}{\Gamma(\alpha_i^\pm + 1) \sin \pi \alpha_i^\pm} \frac{1 \pm e^{-i\pi \alpha_i^\pm}}{2} \left(\frac{s}{s_0}\right)^{\alpha_i^\pm(t)} \quad (4.1)$$

t : fixed

If we assume Mandelstam symmetry⁶⁵⁾ which states $f^\pm(t, J) = f^\pm(t, -J - 1)$ for $J = 1/2, 3/2, \dots$ and further assume $f^\pm(t, J)$ have no poles at positive half-integer values of J , then the reduced residue $r_i^\pm(t)$ should vanish at $J = -3/2, -5/2, \dots$ so that fictitious poles at $J = -3/2, -5/2, \dots$ due to $\Gamma\left(\alpha_i^\pm + \frac{3}{2}\right)$ would actually be absent. Since $\Gamma(\alpha_i^\pm + 1) \times \sin \pi \alpha_i^\pm$ is finite at negative integers, the signature factor $(1 \pm e^{-i\pi \alpha_i^\pm})$ has zeros at negative integers in the wrong signature amplitude (i. e., for even signature amplitude these zeros occur at odd negative integers and for odd signature amplitude at even negative integers). Hence, at the (negative) nonsense values of wrong signature, a Regge trajectory $\alpha(t)$ contributes nothing to scattering amplitude and dips at the corresponding (negative) t -values in angular distribution would follow (since background integral is present, cross section would not exactly vanish there).

Zeros of the same sort should appear also in the case of Fermion Regge poles, which have very important implication for $\pi^\pm p$ backward scattering.

4. 2 Gribov phenomenon^{7), 11)}

It is the well-known fact that for a massless Dirac particle the concept of parity makes no sense even in a theory with parity conservation (as a consequence of γ_5 invariance). Thus the Fermion poles with spin J and parity $(-)^{J \pm 1/2}$ should coincide at $u=0$ ⁷⁾ ($u = (\text{c. m. energy of } \pi N \text{ system in the } u\text{-channel})^2$). More generally, we have MacDowell symmetry for analytically-continued partial-wave amplitudes,¹¹⁾

$$f_{J+1/2}^{J(\pm)}(\sqrt{u}) = -f_{J-1/2}^{J(\pm)}(-\sqrt{u}) \quad (\pm = \text{signature}) \quad (4.2)$$

so that, if a Regge pole $J = \alpha^\pm(\sqrt{u})$ appears in $f_{J-1/2}^{J(\pm)}(\sqrt{u})$, then a corresponding pole at $J = \alpha^\pm(-\sqrt{u})$ should be present in $f_{J+1/2}^{J(\pm)}(\sqrt{u})$. Of course this twin poles have opposite parities. Thus, for $u > 0$, a Fermion trajectory $\alpha(\sqrt{u})$ contains two families of Fermions, one with mass M such that $\alpha(M) = \frac{1}{2}, \frac{5}{2}, \dots$

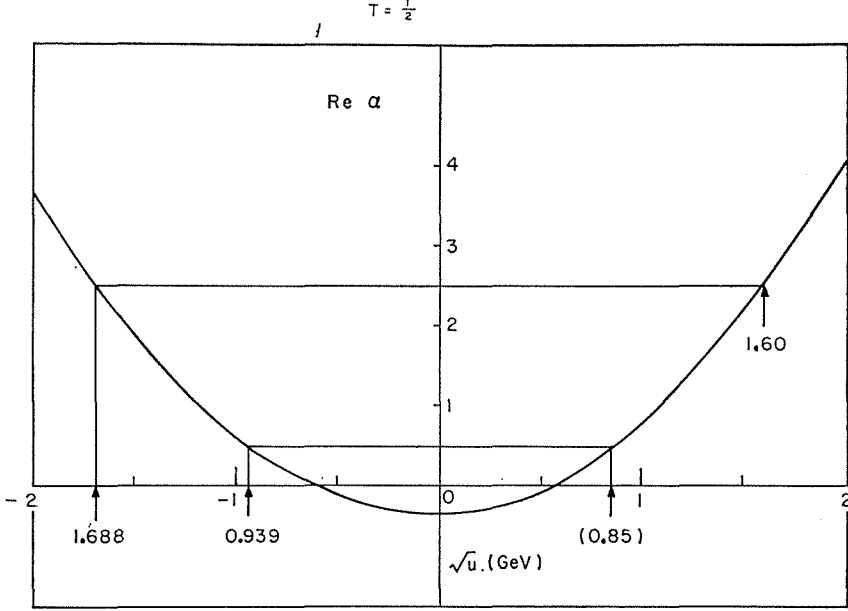


Fig. 2. The nucleon trajectory $\alpha_{Nd}(u)$ as determined by Chiu and Stack (Ref. 6) using a Regge pole fit to backward π^+p scattering data.

or $\frac{3}{2}, \frac{7}{2}, \dots$ and the other with mass M' such that $\alpha(-M')$ has these values. For $u < 0$, the twin poles become each other's complex conjugate ($\alpha(\pm i\sqrt{|u|})$).⁷⁾ This also implies that the trajectory $\alpha(\sqrt{u})$ has the right-hand as well as the left-hand cut, in sharp contrast with the conventional case of Boson trajectory.⁶⁶⁾

Now let us write the πN scattering amplitude in a two-component form :

$$A(\sqrt{s}, u) = f_1(\sqrt{s}, u) + \sigma_r \sigma_i f_2(\sqrt{s}, u) \quad (4.3)$$

where σ_r and σ_i denote nucleon spin components along the final and the initial meson momenta in the s -channel c. m. system, respectively.⁶⁷⁾ Crossing symmetry relates u -channel amplitude $f_{1,2}(\sqrt{u}, s)$ to s -channel one $f_{1,2}(\sqrt{s}, u)$ through¹¹⁾

$$f_1(\sqrt{s}, u) = \frac{E_s + M}{2\sqrt{s}} \left[(\sqrt{u} - \sqrt{s} + 2M) \frac{f_1(\sqrt{u}, s)}{E_u + M} - (\sqrt{u} + \sqrt{s} - 2M) \frac{f_2(\sqrt{u}, s)}{E_u - M} \right] \quad (4.4)$$

and analogous equation for $f_2(\sqrt{s}, u)$. Expand $f_{1,2}(\sqrt{u}, s)$ into partial-wave amplitudes which are to be continued into complex J -plane by the method of Froissart and Gribov and perform Sommerfeld-Watson transform. Picking up Regge poles with dominant contributions, one sees that $f_1(\sqrt{u}, s)$ and $f_2(\sqrt{u}, s)$ contain poles in the amplitudes $f_{J+1/2}^{J(\pm)}(\sqrt{u})$ and $f_{J-1/2}^{J(\pm)}(\sqrt{u})$, respectively. Therefore, according to the foregoing arguments, one concludes that, for each value of u , a Fermion Regge pole contributes twice, through its values $\alpha(\sqrt{u})$ and $\alpha(-\sqrt{u})$, to $f_1(\sqrt{s}, u)$ (and $f_2(\sqrt{s}, u)$).

4. 3 $\pi^\pm p$ backward scattering

It seems natural to suppose that the dominant mechanism for meson-nucleon backward scattering at high energies (say, $p_L > 6$ GeV/c) is the u -channel exchange of baryon octet and decuplet Regge poles. Experiments^{29)~31)} on pion-proton elastic scattering in the backward hemisphere in the energy range $p_L = 4 \sim 17$ GeV/c (for $p_L > 10$ GeV/c only near 180°) show characteristic energy dependence, charge dependence and angular distributions which appear to be fairly well reproduced in Regge pole model (See Figs. 3-11 and 3-12).

Only Δ contributes to $\pi^- p \rightarrow p \pi^-$ while $\pi^+ p$ backward scattering contains all three trajectories N_α , N_τ and $\Delta^{(6)}$ in the u -channel. The contribution of Δ is known to be small from size of the $\pi^- p$ cross section (which is about 1/4 of the corresponding π^+ cross section at 180°) so that it can be neglected in π^+ case.

According to the discussion in 4.1 N_α trajectory has signature zeros at $J = -\frac{1}{2}, -\frac{5}{2}, \dots$ whereas Δ and N_τ have zeros of the kind at $J = -\frac{3}{2}, -\frac{7}{2}, \dots$ ⁶⁾. For

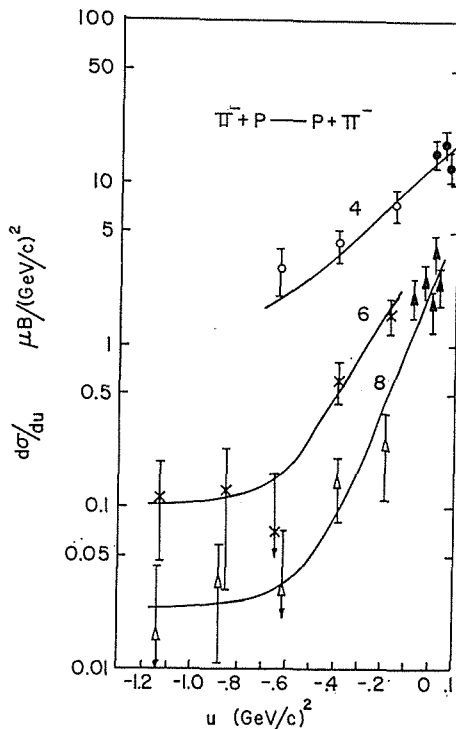


Fig. 3-11. The differential cross section for $\pi^- p$ elastic scattering near the backward direction. Open symbols, H. Brody et al. (Pennsylvania group, Ref. 30); solid symbols, W. R. Frisken et al. (Ref. 30).

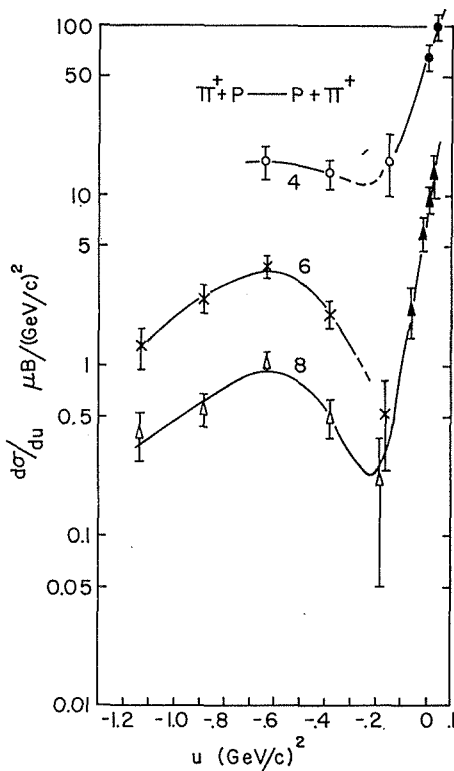


Fig. 3-12. The differential cross section for $\pi^+ p$ elastic scattering near the backward direction. Open symbols, H. Brody et al. (Ref. 30); solid symbols, Frisken et al. (Ref. 30).

small negative values of u , N_a is known⁶⁸⁾ to pass through $J = -\frac{1}{2}$ ("nonsense transition of unphysical signature"), but Δ and N_r do not seem to go through their first nonsense value of wrong signature ($J = -\frac{3}{2}$) for such small u .

Taking into account Gribov phenomenon discussed in 4.2 nucleon trajectory may develop a dip in angular distribution near the value of u where both $\alpha_{N_a}(\sqrt{u})$ and $\alpha_{N_a}(-\sqrt{u})$ are near $J = -\frac{1}{2}$ if it is the main contributor. Since a dip has been observed near $u = -0.2$ (GeV/c)² in $(d\sigma/d\Omega)_{\pi^+p}$ ²⁹⁾ and the contribution of N_r , if it were large, masks a predicted dip due to N_a , Chiu and Stack⁶⁾ assumed that N_r couples weakly to πN system and neglected it altogether.

From the best fit to the π^+p data ($p_L = 4 \sim 10$ GeV/c) Chiu and Stack⁶⁾ obtained for the trajectory function.

$$\alpha_{N_a}(\sqrt{u}) = -0.340 + 0.093\sqrt{u} + 1.052u$$

which is shown in Fig. 2. Note that a $\frac{1}{2}$ -baryon of mass 850 MeV lying on it corresponds to no observed particle so that residue must vanish there.

Including the data at $u=0$ up to $p_L = 17$ GeV/c, Ashmore et al.³¹⁾ obtain

$$\begin{aligned}\alpha_\Delta(0) &= -0.14 \pm 0.06, \\ \alpha_N(0) &= -0.20 \pm 0.05.\end{aligned}$$

Another charge dependence of pion-proton backward scattering is that, in the region of $u \geq -0.06$ (GeV/c)², the π^- backward peaks are several times wider than π^+ backward peaks and each appears to go through a maximum before reaching 180°. The maxima seem to occur at about $u = -0.05$ (GeV/c)².³¹⁾

Final remark will be concerned with spin dependence of $\pi^\pm p$ amplitude near backward directions. As noted by Stack,⁶⁶⁾ because of Gribov phenomenon, a significant polarization in π^-p scattering is expected although only Δ trajectory can contribute to π^-p . This would provide an interesting test for our model.

4. 4 $K^\pm p$ backward scattering⁶⁹⁾

Several groups^{15), 32), 69)} reported the experimental results on $K^\pm p$ elastic scattering near the backward direction in a few GeV region. The data are shown in Figs. 3-13 and 3-14. In this energy region the resonance effects in the direct channel are also important. The interference between resonance and Regge pole amplitudes has been studied by Barger and Cline⁶⁸⁾ for πp backward and π^-p charge exchange scatterings. For K^+p backward scattering, however, there seems no significant evidence for a large contribution from the excited high-spin hyperon states in the direct channel. This observation is based on the two experimental facts: 1) At present there are many well-known low- as well as high-mass $Y=0$ baryon states while the situation is less clear regarding $Y=2$ states, and 2) the K^+p cross section near 180° is much larger than that for K^-p scattering. In fact the upper limit for the $d\sigma(K^-p)/d\Omega$ near $\cos\theta = -1$ is estimated by Cline et al.⁶⁹⁾ to be smaller than $1\mu b/\text{ster}$ whereas $d\sigma(K^+p)/d\Omega$ goes up to about $20\mu b/\text{ster}$ near backward direction. Moreover, there is a possible turnover near $u \leq 0$ in the K^+p momentum-transfer distribution. This phenomenon could be explained if the Λ_c exchange dominates K^+p backward scattering and the Λ_c trajectory has a slight curvature so as to intersect the nonsense spin

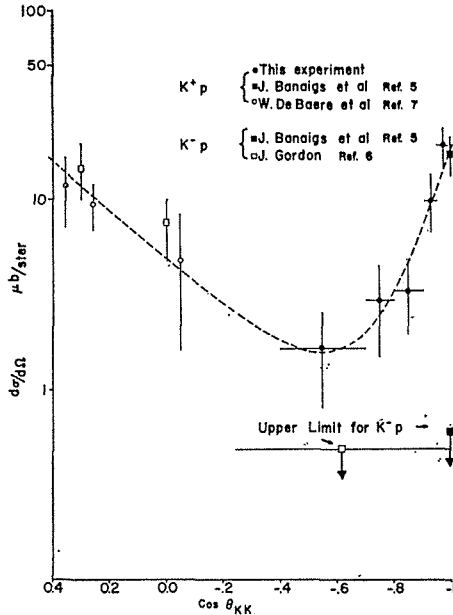


Fig. 3-13. Differential cross section for K^+p elastic scattering near $\cos\theta=-1$ for the laboratory beam momentum of ~ 3.5 GeV/c. The data are from Ref. 69 (\bullet); Ref. 32 (\blacksquare); Ref. 15 (\circ). Also shown are the present upper limits on the differential cross section for K^-p elastic scattering in the backward hemisphere. Open squares with error bars are the K^-p cross section reported by J. Gordon, Phys. Letters 21, 117 (1966). The dashed curve is drawn to guide the eye.

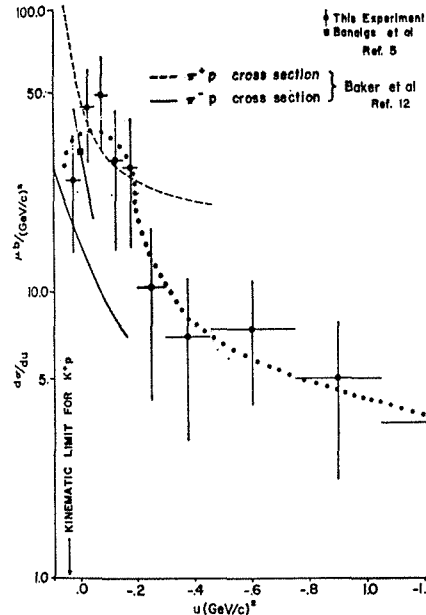


Fig. 3-14. Differential cross section as a function of u for K^+p elastic scattering at a beam momentum of 3.53 GeV/c. With error bars: solid circles, Ref. 69; solid squares, Ref. 32. Also shown are the differential cross sections for π^+p and π^-p near $u=0$ for beam momentum of 3.55 GeV/c (W. F. Baker et al., Phys. Letters 23, 605 (1966)). The dotted line is drawn through the K^+p data points to guide the eye.

value of $-\frac{1}{2}$ near $u=0$ when extrapolated from the region $u>0$.

§ 5. Polarization and possible non-Regge-pole effects

So far we have concentrated our attention upon the angular distributions and their energy dependence so that the spin dependence of high energy amplitudes was not a primary interest. Nonetheless we have encountered the so-called helicity-flip phenomena that originate from the fact that the ρ and A_2 mesons are not fixed but moving poles in the complex J -plane. From this we further argue that Regge pole exchange amplitude has its own characteristic spin dependence and that to study the spin structure of the interference terms between Regge amplitudes may provide a critical test of Regge pole model when compared with detailed experimental observations. Fundamental physical quantities of interest in the spin dependence of scattering amplitudes are polarization

parameters of recoil nucleons and decay correlations or spin density matrices of produced resonances. Our main interest in this section is polarizations of the reactions $\pi^\pm p \rightarrow \pi^\pm p$ and $\pi^- p \rightarrow \pi^0 n$. We shall study decay correlations in the next section.

5.1 Experimental results

The recent data reported by CERN group⁷⁰⁾ on the polarization parameter $P(\theta)$ for $\pi^\pm p$ elastic scattering in the energy range from $p_L=6$ to 12 GeV/c show the characteristic charge and angular dependences:

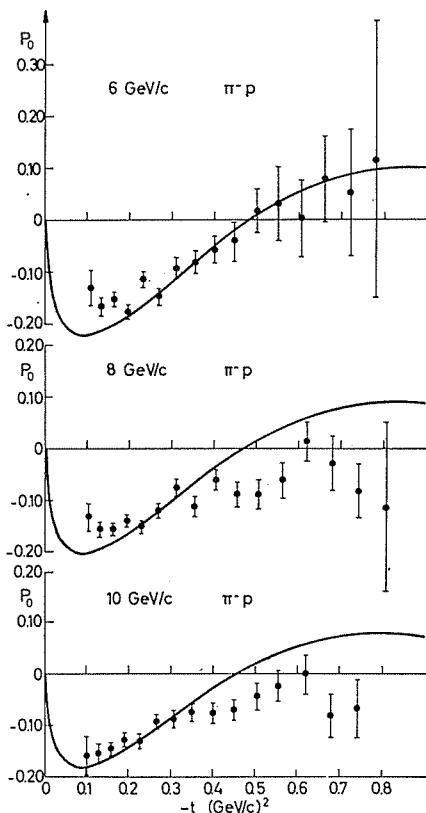


Fig. 4. The polarization parameter P_0 versus t in $\pi^\pm p$ elastic scattering reported by M. Borghini et al. (Ref. 70). The curves represent the theoretical predictions of Chiu et al. (Ref. 71).

- (1) $P(\pi^+p)$ and $P(\pi^-p)$ have opposite signs and approximately equal absolute values.
- (2) The small absolute values of P at $-t = 0.6$ (GeV/c)².
- (3) $P(\pi^+p)$ appears to decrease with increasing energy, while $P(\pi^-p)$ has no visible energy variation.

Maximum polarization of about 15% occurs near $-t = 0.2$ (GeV/c)².

Polarization parameter for the reaction $\pi^- p \rightarrow \pi^0 n$ were measured by Bonamy et al.³⁹⁾ with polarized proton targets and the result indicates about 15% polariza-

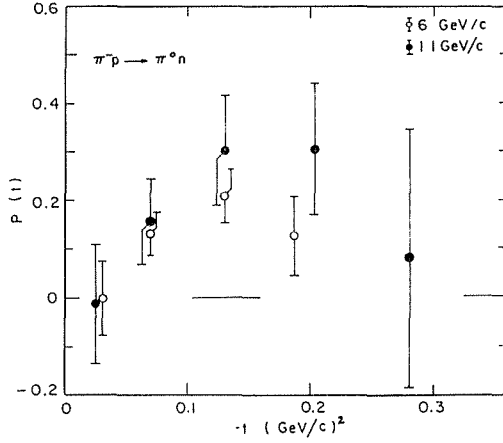


Fig. 5. Polarization parameter $P_0(t)$ at 5.9 GeV/c (open circles) and 11.2 GeV/c (solid circles) for the reaction $\pi^- p \rightarrow \pi^0 n$, measured by Bonamy et al. (Ref. 39).

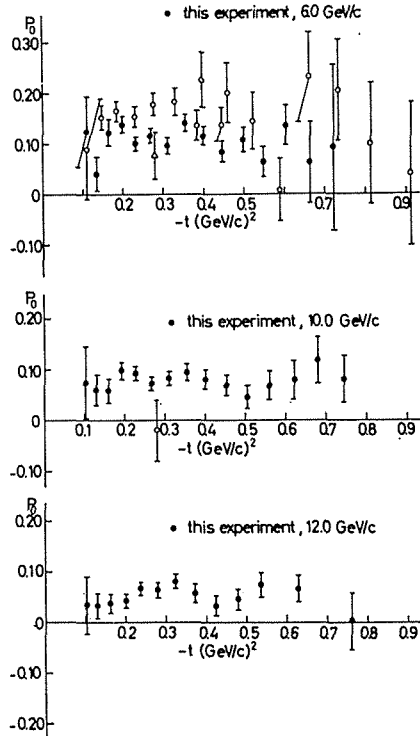


Fig. 6. The polarization parameter P_0 versus t in pp elastic scattering. This experiment refers to the data of the CERN group (Ref. 70). In (a), open circles, 5.9 GeV/c (P. Grannis et al., Phys. Rev. 148, 1297 (1966)); open triangle, 5.8 GeV/c (V. P. Kanavets et al., Soviet Phys. -JETP 18, 874 (1964)). In (b), open circle, 9.4 GeV/c (Kanavets et al.)

tion in contradiction to the single ρ Regge pole model. The data at $p_L=5.9$ and 11.2 GeV/c are shown in Fig. 5. The polarizations averaged over all data are,

$$\begin{aligned} \langle P \rangle &= (14 \pm 3.5)\% \quad \text{for } 0.02 \leq |t| \leq 0.24 \text{ (GeV/c)}^2 \text{ at } 5.9 \text{ GeV/c} \\ \langle P \rangle &= (12 \pm 4)\% \quad \text{for } 0.015 \leq |t| \leq 0.34 \text{ (GeV/c)}^2 \text{ at } 11.2 \text{ GeV/c} \end{aligned}$$

We note that there is no significant energy dependence in this case. Finally we show in Fig. 6 polarization data on pp scattering at 6, 10 and 12 GeV/c and the reaction, $\pi^+p \rightarrow \Sigma^+K^+$ at 3.23 GeV/c (Fig. 7).

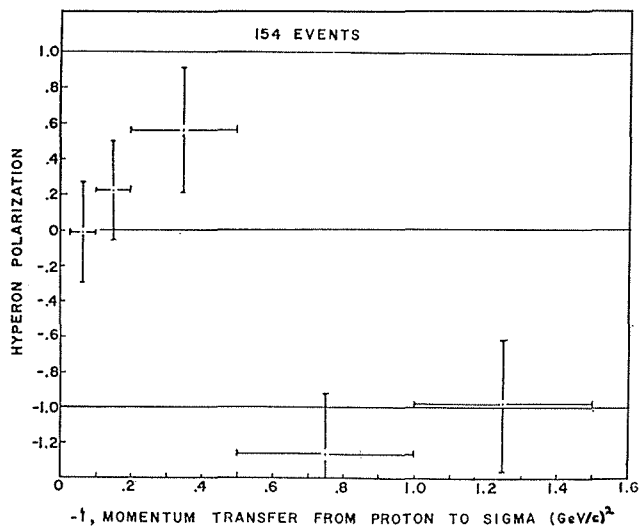


Fig. 7. The Σ^+ polarization as a function of t for the reaction $\pi^+p \rightarrow \Sigma^+K^+$ at 3.23 GeV/c, as measured by Kofler et al, quoted by L. Van Hove in B. Measurements based on 154 events.

5. 2 Pure Regge pole model

Chiu, Phillips and Rarita analyzed the $\pi^\pm p$ data in terms of three Regge poles (P , P' , ρ) and obtained fairly good agreement with experiment. Let us write the πN scattering amplitude in the form

$$A(s, t) = f(s, t) + i g(s, t) \vec{\sigma} \cdot \vec{n} \quad (5.1)$$

where \vec{n} is a unit vector normal to the scattering plane and f and g are spin non-flip and flip amplitudes, respectively. Then,

$$\frac{d\sigma}{d\Omega} = |f|^2 + |g|^2, \quad (5.2)$$

$$P(\theta) \frac{d\sigma}{d\Omega} = 2 \text{Im}(f^*g). \quad (5.3)$$

From Eq. (1.1) one finds

$$\begin{aligned} P(\theta) \frac{d\sigma}{d\Omega}(\pi^\pm p \rightarrow \pi^\pm p) &= 2 \text{Im}[\pm (f_P^* + f_{P'}^*) g_\rho \\ &\quad \pm f_\rho^* (g_P + g_{P'}) + f_P^* g_{P'} + f_{P'}^* g_P]. \end{aligned} \quad (5.4)$$

Since ρ couples strongly to spin-flip part g and P and P' mainly to nonflip part f , the second term in the RHS of Eq. (5.4) can be neglected compared with the first term. Furthermore, in order to account for the observed charge dependence (i. e., the reversal of sign of $P(\theta)$ between π^-p and π^+p), the last term should also be small compared with the first. With these simplifications, one has

$$P(\theta) \frac{d\sigma}{d\Omega}(\pi^\pm p \rightarrow \pi^\pm p) = \pm 2 \operatorname{Im}(f_P^* + f_{P'}^*) g_\rho. \quad (5.5)$$

This explains roughly why $P(\theta) \sim 0$ near $-t = 0.6$ (GeV/c)² since g_ρ vanishes there (see Sec. 3). As for s -dependence of $P(\theta)$, we have from (5.5)

$$P(\theta) \propto s^{-(\alpha_p(t) - \alpha_\rho(t))}$$

If Pomeranchon has a small slope, we have approximately

$$P(\theta) \propto s^{-(1/2 \sim 2/3)} \text{ near its maximum around } -t = 0.2 \text{ (GeV/c)}^2.$$

As mentioned in 5.1, (3), π^-p data have no such a visible energy dependence. If this will be confirmed by detailed experiment, we must face with difficulties in the Regge pole model.

In the charge exchange scattering we have trouble with experiment. Single ρ Regge pole exchange model predicts $P(\theta) = 0$, whereas experiment indicates a polarization of about 15%. Explanations of this phenomenon have been attempted within the frame of refined Regge pole models. In any case, the ρ pole model is accepted as a first-order approximation in the description of the reaction $\pi^-p \rightarrow \pi^0n$.

5.3 Modified Regge pole model for π^-p charge exchange scattering

5.3.1 $\rho + \rho'$ model⁷²⁾

Recent analysis of Högaasen and Fisher⁷³⁾ of nucleon-nucleon charge exchange scattering at high energy indicates that, in addition to ρ pole, the another pole ρ' is needed to explain the data of the forward differential cross section and the total cross section consistently.⁷⁴⁾

Taking into account the contribution of ρ' pole, the scattering amplitude of the π^-p charge exchange process can be expressed as ;

$$\begin{cases} f = f_\rho + f_{\rho'} , \\ g = g_\rho + g_{\rho'} , \end{cases} \quad (5.6)$$

where the formula for $f_{\rho'}$ ($g_{\rho'}$) is identical to that for f_ρ (g_ρ) except for the appearance of the primed quantities in residue and trajectory functions. The results calculated by Logan et al.⁷²⁾ are shown in Fig. 8.1. The rough s dependence is estimated from $\alpha_{\rho'}$ and α_ρ :

$$P_0 \sim \frac{s^{\alpha_\rho + \alpha_{\rho'}}}{s^{2\alpha_\rho}} \sim s^{\alpha_{\rho'} - \alpha_\rho} \sim s^{-0.33}, \quad (5.7)$$

which decreases with energy in contradiction to the existing data.

5.3.2 $\rho +$ direct channel resonance model⁷⁵⁾

At intermediate energies, Barger and Cline⁶⁸⁾ suggest that the amplitude due

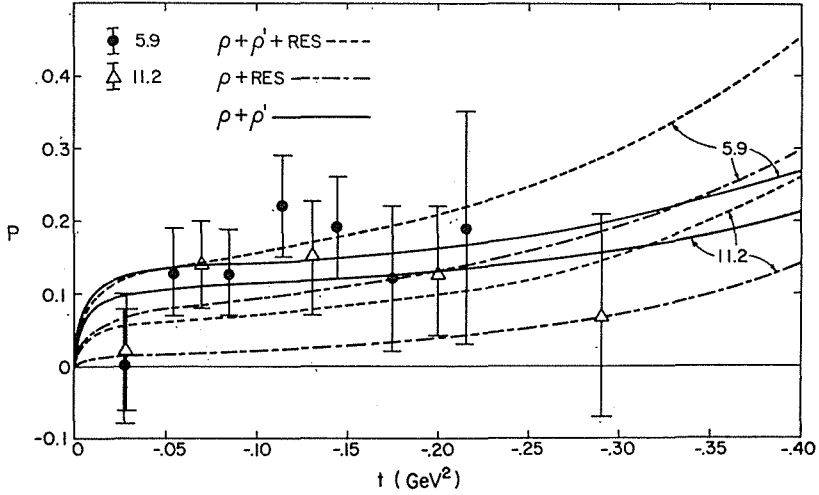


Fig. 8-1. The fit of the polarization data on the reaction $\pi^-p \rightarrow \pi^0n$ at 5.9 and 11.2 GeV/c with models discussed in the text (§§ 5.3), as calculated by Logan et al. (Ref. 72). Solid lines are predictions of $\rho + \rho'$ model; dashed-dotted lines, ρ +direct channel resonance model; dotted lines, $\rho + \rho'$ +resonance model. The numbers associated with the curves represent the laboratory-system momenta. Data are from Ref. 70 (● 5.9 GeV/c and \triangle 11.2 GeV/c).

to crossed-channel exchange is roughly the same size as the amplitude due to direct channel resonances. According to them, the polarization in π^-p charge exchange scattering may be explained in terms of the interference of the Regge pole amplitude with the low-lying Fermion resonances in the direct channel. In this model

$$\begin{cases} f = f_\rho + f_{res}, \\ g = g_\rho + g_{res}, \end{cases} \quad (5.8)$$

$$\begin{pmatrix} f_{res} \\ g_{res} \end{pmatrix} = -\frac{\sqrt{2}}{2q} \sum_{l,i} (-)^{l+1/2} \begin{pmatrix} (J+1/2)P_l(\cos\theta_s) \\ (-1)^{J-1-1/2}P'_l(\cos\theta_s) \end{pmatrix} \cdot \frac{\eta_i}{E - E_i + i\Gamma_i/2} \quad (5.9)$$

where E , J , l , E_i , Γ_i and η_i are the total c.m. energy, the total spin, orbital angular momentum, energy, width and elasticity of the resonances, respectively. Consider the contribution of all the known resonances to f_{res} . The spin and parity assignment for the higher resonances recently observed is made on the basis of a Regge recurrence scheme.⁶⁸⁾ (These assignments were tested in two separate analyses of π^-p elastic scattering at 180° and π^-p charge exchange at 0°)

The calculated results are shown in Fig. 8.1.

The polarization in this case is roughly proportional to f_{res}/f_{Reg} , and the decrease of $P(\theta)$ with energy arises from the fact that f_{res} decreases faster with energy than f_{Reg} . The amplitude f_{Reg} decreases exponentially with $-t$ whereas f_{res} decreases less rapidly, hence $P(t)$ increase as $-t$ increases.

5. 3. 3 ρ + Regge cut model⁷⁶⁾

The existence of the cuts in the angular momentum plane have been discussed

by several authors from the theoretical point of view⁷⁷⁾ At present time we have not yet get clear-cut conclusion about the existence of the cuts since a theoretical estimate is prohibitively difficult to make.

Here we introduce, phenomenologically, the leading cut associated with ρ and P exchange, the branch point of which is given by,

$$\alpha_c(t) = \alpha_\rho \left[\left(\frac{\alpha_\rho'}{\alpha_\rho' + \alpha_P'} \right)^2 t \right] + \alpha_P \left[\left(\frac{\alpha_P'}{\alpha_\rho' + \alpha_P'} \right)^2 t \right] - 1, \quad (5.10)$$

where $\alpha_\rho(t)$ and $\alpha_P(t)$ are the ρ and P trajectories and α_ρ' (α_P') are their slopes (which are assumed to be constant.)

Carrying out the Sommerfeld-Watson transformation, f and g will be given asymptotically by,

$$\begin{pmatrix} f \\ g \end{pmatrix} = \int dJ \begin{pmatrix} c_1 \\ c_2 \end{pmatrix} \left(\frac{E}{E_0} \right)^J \left(\tan \frac{\pi J}{2} + i \right) \quad (5.11)$$

where c_1 and c_2 are reduced discontinuities across the cut of the spin non-flip and flip amplitudes with the threshold dependence $(p^t_i p^t_{i'})^J$ factored out.

For (E/E_0) large enough, the rough estimation will be given by the following form ;

$$\begin{pmatrix} f \\ g \end{pmatrix} \sim (E/E_0)^{\alpha_c(t)} \frac{1}{\log(E/E_0)}. \quad (5.12)$$

The energy dependence of the polarization will be given ;

$$P(E, t) \sim E^{(\alpha_c(t) - \alpha(t))} / (E_0)^{\alpha_c(t)} (E_0)^{\alpha_P(t)} \quad (5.13)$$

and

$$\alpha_c(t) - \alpha_\rho(t) = - \frac{\alpha_\rho'^2}{\alpha_\rho' + \alpha_P'} t > 0 \quad \text{for } t < 0 \quad (5.14)$$

Thus this model predicts a polarization which increases with energy.

5. 3. 4 ρ + absorption model⁷⁸⁾

It has been pointed out by several authors⁷⁹⁾ that Regge pole model leads to difficulties in connection with the t -dependence of the two-body amplitudes whereas absorption model do not explain their s dependence. From a purely phenomenological point of view, the combination of the two approaches might give both the right s and t dependence of the scattering amplitudes. The formulation is done using the F -matrix (overlap matrix) introduced by Bialas and Van Hove.⁸⁰⁾

The two-body scattering amplitude is expressed as ;

$$\begin{aligned} A_{ji}(s, t) = & \mathfrak{N}^{(a)}(s, \vec{q}_i \cdot \vec{q}_j) \delta_{ji} + R_{ji}^{(a)}(s, \vec{q}_i \cdot \vec{q}_j) \\ & + 2i \int d\vec{p} \mathfrak{N}^{(a)}(s, \vec{q}_j \cdot \vec{p}) R_{ji}^{(a)}(s, \vec{p} \cdot \vec{p}_j), \end{aligned} \quad (5.15)$$

where $\mathfrak{N}^{(a)}(s, \vec{q}_i \cdot \vec{q}_j)$ represents the shadow scattering amplitudes and $R_{ji}(s, \vec{q}_i \cdot \vec{q}_j)$ is the Regge amplitude. The suffix (a) means that we take particular model, according to which the overlap matrix which represents the contribution of the n -particle states ($n > 2$) is assumed to be diagonal⁸⁰⁾ with respect to channel

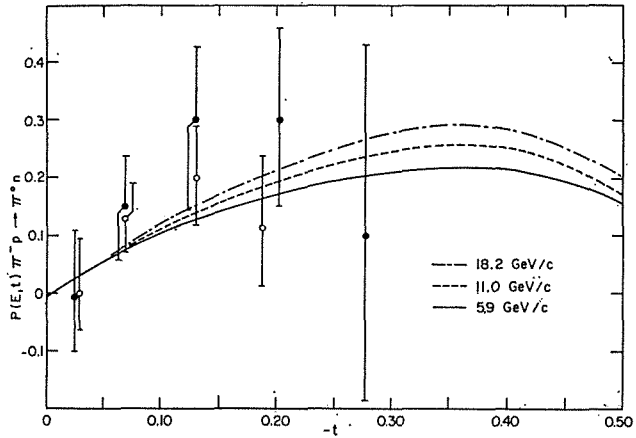


Fig. 8-2. Comparison of the one-pole plus one-cut model with experiment, as calculated by Lany et al. (Ref. 76). The closed circles are data at 11 GeV/c; open circles, data at 5.9 GeV/c, both from Ref. 70.

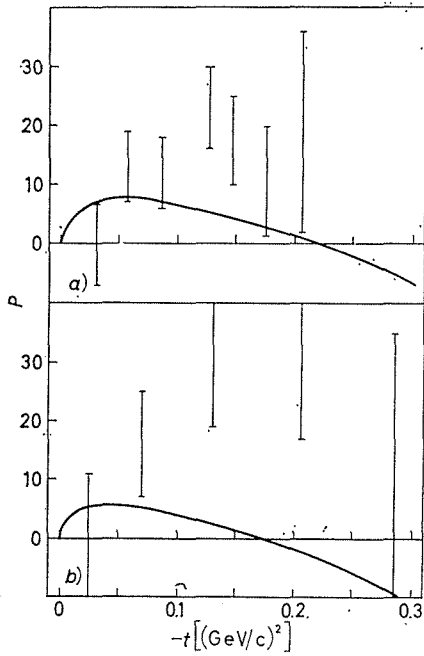


Fig. 8-3. Recoil neutron polarization in $\pi^-p \rightarrow \pi^0n$ reaction at a) 6 and b) 11 GeV/c, as obtained by a ρ^+ absorption model (Ref. 78). A purely \mathcal{N} -function is assumed (See Eq. (5.16) in Sec. 5). Data from Ref. 39.

indices i and j . The third term represents overlap integral of the two amplitudes. (If the particle has spin, then we must make sum with the helicities of the intermediate two-body states.) For large s and $t=0$, one has the asymptotic behaviours

$$\begin{aligned} \mathfrak{A}^{(a)}(s, 0) &\sim \text{const } e^{R^2 t}, \\ R^{(a)}(s, 0) &\sim \text{const} \cdot s^{\alpha(t)} \quad (\alpha < 1), \end{aligned} \quad (5.16)$$

then the third term can be calculated;

$$\text{the third term} \sim \text{const} \frac{R^2 + \alpha \ln s}{s^\alpha}. \quad (5.17)$$

For the π - p charge exchange process, the third term contributes in addition to the ρ trajectory exchanged term ($R_{ji}(s, \vec{q}_i \cdot \vec{q}_j$)).

The calculated results are shown in Fig. 8-3. Note that the third term has the same form as the one of the contribution from the process exchanged a branch point trajectory in the complex angular momentum plane.

§ 6. Resonance production and decay correlation

In this section we investigate the decay correlations of resonances produced in the reactions of the type

$$a + b \longrightarrow c + d \quad (6.1)$$

where one or both of the final systems are dynamically unstable. Experimentally these reactions occur with relatively small momentum transfers, indicating the peripheral nature of the production mechanism. In a peripheral model (like one particle exchange one) the production amplitude and the decay angular correlations of resonances d and/or c depend on the dynamical properties of the exchanged objects⁸¹⁾. In the following we suppose that the production processes (6.1) proceed mainly via the scheme

$$a + \bar{c} \longrightarrow Z \longrightarrow d + \bar{b} \quad (6.1)'$$

in the crossed channel, where Z is the exchanged object (assumed to be Regge pole).

For the time being let us suppose that d is dynamically unstable, decaying into two particles α and β , where α and β have spins S_α and S_β , respectively, whereas c is stable (like nucleon). Let us first evaluate the angular distribution of the decay $d \rightarrow \alpha + \beta$ in the rest frame of the d when the d has spin component m along the polar axis specified below. If the particle α is emitted in the direction (θ, φ) (so that β in the direction $(\pi - \theta, \pi + \varphi)$), the decay matrix element is

$$M_m^{S_d}(\lambda_\alpha, \lambda_\beta) = \sqrt{\frac{2S_d + 1}{4\pi}} d_{m\lambda}^{S_d}(\theta) \exp\{i\varphi(m - \lambda)\} M_d(\lambda_\alpha, \lambda_\beta), \quad (6.2)$$

where S_d , λ_α and λ_β are the spin of the d , helicities of α and β , respectively and $d_{m\lambda}^{S_d}(\theta)$ is the reduced rotation matrix with $\lambda = \lambda_\alpha - \lambda_\beta$. $M_d(\lambda_\alpha, \lambda_\beta)$ depends on the decay mechanism and if the decay conserves parity, it has the following symmetry property:

$$M_d(\lambda_\alpha, \lambda_\beta) = \eta_\alpha \eta_\beta \eta_d (-1)^{S_\alpha - S_\alpha - S_\beta} M_d(-\lambda_\alpha, -\lambda_\beta), \quad (6.3)$$

where η_α , η_β and η_d are intrinsic parities of the particles α , β and d , respectively. If α and β are both spinless, or if $s_\alpha=1/2$ and $s_\beta=0$, there is only one constant M_d characterizing the decay. Now the angular distribution of the true final particles α and β in

$$a+b \longrightarrow c+d \longrightarrow c+\alpha+\beta \quad (6.1)''$$

is expressed as⁸¹⁾

$$W(\theta, \varphi) \propto \sum_{\substack{\lambda_\alpha \lambda_\beta \\ mm'}} |M_d(\lambda_\alpha \lambda_\beta)|^2 \exp[i(m-m')\varphi] d_{m\lambda}^{S_d}(\theta) d_{m'\lambda}^{S_d}(\theta) \rho_{mm'}^d, \quad (6.4)$$

where it is assumed that in the rest frame of the d the particle α is emitted in the direction (θ, φ) with the polar axis being the spin quantization axis of the d . In Eq. (6.4), $\rho_{mm'}^d$ is called the spin density matrix of the d , in which information on the production mechanism (i. e., the dynamical properties of the system Z and its coupling to the initial and the final states of the crossed channel (6.1)) is included, and will be defined below in terms of the production amplitudes. Thus we can get the knowledge of the spin dependence of the production amplitudes to the extent that can be determined by the decay angular distributions.

6.1 Density matrix and decay correlation

As usual we define the s-channel center of mass frame helicity amplitudes⁸²⁾ for the reaction (6.1), denoting them by

$$\langle \lambda_c \lambda_d | f^s(s, t) | \lambda_a \lambda_b \rangle \equiv f^{s, \lambda_c \lambda_d; \lambda_a \lambda_b}(s, t)$$

where λ 's denote the helicities. We choose as spin quantization axis (z -axis) for d the direction of the momentum of b in the rest frame of d (which we call the d reference frame henceforth). Denoting by m the spin projection of the d along this quantization axis, we can write

$$\begin{aligned} \langle \lambda_c m | f^s(s, t; \vec{p}_d=0) | \lambda_a \lambda_b \rangle \\ = \sum_{\lambda_d} \langle m | \lambda_d \rangle \langle \lambda_d \lambda_c | f^s(s, t; \vec{p}_d=0) | \lambda_a \lambda_b \rangle, \end{aligned} \quad (6.5)$$

where of course λ_d is the helicity of d in the c. m. system. The rotational matrix element $\langle m | \lambda_d \rangle$ corresponds to the rotation in the rest frame of d (designated by O_d) from the helicity direction $\vec{p}_a = -\vec{p}_c$ to the quantization axis \vec{p}_b and is expressed as

$$\langle m | \lambda_d \rangle = \langle \lambda_d | m \rangle = d_{\lambda_d m}^{S_d}(-\phi_d), \quad (6.6)$$

with

$$\tan \phi_d = \frac{M_d}{E_d} \sqrt{1 - \cos^2 \theta_s} \left(\cos \theta_s - \frac{v_d}{v_b} \right)^{-1}, \quad (6.7)$$

where E_d, v_d, v_b , and M_d are the c. m. energy of d , velocities of d and b in the c. m. system and the mass of d , respectively. The density matrix element of the resonance d is defined by

$$\rho_{mm'}^d = \frac{\sum_{\lambda_a \lambda_b \lambda_c} \langle \lambda_c m | f^s(s, t; \vec{p}_d=0) | \lambda_a \lambda_b \rangle \langle \lambda_c m' | f^s(s, t; \vec{p}_d=0) | \lambda_a \lambda_b \rangle^*}{\sum_{\lambda_c} |\langle \lambda_c \lambda_d | f^s(s, t) | \lambda_a \lambda_b \rangle|^2}, \quad (6.8)$$

which has the following properties by definition and reflexion invariance :

$$(i) \quad \sum_m^d \rho_{mm}^d = 1 \quad (T_r(\rho_{mm}^d) = 1), \quad (6.9a)$$

$$(ii) \quad \rho_{mm'}^d = \left(\rho_{m'm}^d \right)^* \quad (\text{hermitian}), \quad (6.9b)$$

$$(iii) \quad \rho_{mm'}^d = (-)^{m-m'} \rho_{-m-m'}^d. \quad (6.9c)$$

One easily sees that the independent elements of the density matrix are $S_d(S_d + 2)$ for integer S_d and $\left(S_d + \frac{1}{2}\right)\left(S_d + \frac{3}{2}\right) - 1$ for half-integer S_d of which the diagonal elements are real.

When (6.1) is analyzed by the mechanism (6.1)', it is convenient to express the spin density matrix in terms of the t -channel c. m. helicity amplitudes through the Trueman-Wick crossing symmetry.⁸³⁾ The result is⁸¹⁾

$$\rho_{mm'}^d = \frac{\sum_{\lambda_a \lambda_b \lambda_c} \langle m \bar{\lambda}_b | f^t(s, t) | \bar{\lambda}_c \lambda_a \rangle \langle m' \bar{\lambda}_b | f^t(s, t) | \bar{\lambda}_c \lambda_a \rangle^*}{\sum_{\lambda'_s} \langle \lambda_a \bar{\lambda}_b | f^t(s, t) | \bar{\lambda}_c \lambda_a \rangle \langle \lambda_a \bar{\lambda}_b | f^t(s, t) | \bar{\lambda}_c \lambda_a \rangle^*}, \quad (6.10)$$

where use has been made of

$$\sum | \langle \lambda_c \lambda_a | f^s(s, t) | \lambda_a \lambda_b \rangle |^2 = \sum | \langle \lambda_a \lambda_b | f^t(s, t) | \lambda_c \lambda_a \rangle |^2, \quad (6.11)$$

which is a consequence of the orthogonality of the T-W crossing matrices. It is shown by Gottfried and Jackson⁸¹⁾ that the density matrix has the following properties according to the spin and parity of the exchanged system Z if parity is conserved in the t -channel :

- (i) In the case of the scalar exchange process (spin of $Z=0$), $\rho_{mm'}^d = 0$ for $m, m' > S_d$. This comes from the angular momentum conservation in the final vertex of the t -channel. The Treiman-Yang test is one of the simplest cases ($S_d=0$).
- (ii) In the production of a resonant state of natural (unnatural) parity from an incident pseudoscalar meson, if Z has natural (unnatural) parity, then $\rho_{mm'}^d = 0$ for m or $m' = 0$. Here the "natural" parity means parity is $(-)^s$, where s is the spin of the particle.

To what extent the decay angular distribution (6.4) gives us information on the density matrix? The reflexion invariance of the decay interaction and the production mechanism implies

$$\begin{cases} W(\theta, \varphi) = W(\pi - \theta, \pi + \varphi), \\ W(\theta, \varphi) = W(\theta, -\varphi), \end{cases} \quad (6.12)$$

and the reality of $W(\theta, \varphi)$ leads to

$$W(\theta, \varphi) \propto \sum_{\substack{\lambda_a \lambda_\beta \\ mm'}} |M_a(\lambda_a \lambda_\beta)|^2 \cos[(m-m')\varphi] R_e \rho_{mm}^d d_{m\lambda}^{S_d}(\theta) d_{m'\lambda}^{S_d}(\theta). \quad (6.13)$$

Thus the imaginary parts of the density matrices do not appear in the decay distribution and we can get information only on the real parts of the density matrices due to the parity conservation in the decays. The imaginary parts would occur in the decay distribution if the particle decays through a parity

violating interaction.

When both of the final systems in the reaction (6.1) are unstable, the angular distributions of their decay products provide more detailed information on their production mechanism.⁸⁴⁾ Advantage can be taken of the Lorentz transformation properties of the helicity amplitudes,

$$\begin{aligned} \langle m, n | f^s(s, t; \vec{p}_d = \vec{p}_c = 0) | \lambda_a \lambda_b \rangle \\ = \sum_{\lambda_c \lambda_d} \langle m | \lambda_c \rangle \langle n | \lambda_d \rangle \langle \lambda_c \lambda_d | f^s(s, t; \vec{p}_d = \vec{p}_c = 0) | \lambda_a \lambda_b \rangle, \end{aligned} \quad (6.14)$$

where m and n are the spin components along the respective quantization axes in the c and d reference frames, respectively. The joint density matrix is defined by⁸⁴⁾

$$\rho_{nn'}^{mm'} = \frac{\sum_{\lambda_a \lambda_b} \langle mn | f^s(s, t; \vec{p}_d = \vec{p}_c = 0) | \lambda_a \lambda_b \rangle \langle m' n' | f^s(s, t; \vec{p}_d = \vec{p}_c = 0) | \lambda_a \lambda_b \rangle^*}{\sum_{\lambda'_a} \langle \lambda_c \lambda_d | f^s(s, t) | \lambda_a \lambda_b \rangle \langle \lambda_c \lambda_d | f^s(s, t) | \lambda_a \lambda_b \rangle^*}. \quad (6.15)$$

The individual density matrices of c or d are obtained by summing over the magnetic substates of c or d :

$$\left\{ \begin{array}{l} \rho_{mm'} = \sum_n \rho_{nn}^{mm'}, \\ \rho_{nn'} = \sum_m \rho_{mm}^{nn'}. \end{array} \right. \quad (6.16)$$

The joint density matrix (6.15) has the following properties;

$$(i) \quad \sum_{mn} \rho_{nn}^{mm} = \sum_m \rho_{mm} = \sum_n \rho_{nn} = 1 \quad (T_r \rho = 1) \quad (6.17a)$$

$$(ii) \quad (\rho_{nn'}^{mm'})^* = \rho_{n'n}^{m'm} \quad (\text{hermitian}) \quad (6.17b)$$

$$(iii) \quad \rho_{-n-n'}^{-m-m'} = (-)^{(m-m')+(n-n')} \rho_{nn'}^{mm'} \quad (\text{reflexion symmetry}) \quad (6.17c)$$

From these one easily finds

$$(iv) \quad \rho_{nn}^{mm} \text{ is real,}$$

and

$$(v) \quad \rho_{n-n}^{m-m} \text{ is real if } 2(n-m) \text{ is even integer and purely imaginary if } 2(n-m) \text{ is odd.}$$

The distribution describing simultaneously the two-body decay of the c in its rest frame and the two-body decay of the d in its rest frame is obtained

$$W(\theta_c \varphi_c; \theta_d \varphi_d) = \sum_{mm'} M_{mm'}^{S_d}(\theta_d \varphi_d) M_{nn'}^{S_c}(\theta_c \varphi_c) \rho_{nn'}^{mm'}, \quad (6.18)$$

where

$$M_{mm'}^{S_d}(\theta_d \varphi_d) = \sum_{\lambda_a \lambda_\beta} M_m^{S_d}(\lambda_a \lambda_\beta) M_{m'}^{S_d*}(\lambda_a \lambda_\beta), \quad (6.19a)$$

$$M_{nn'}^{S_c}(\theta_c \varphi_c) = \sum_{\lambda_a' \lambda_{\beta'}} M_n^{S_c}(\lambda_a' \lambda_{\beta'}) M_{n'}^{S_c*}(\lambda_a' \lambda_{\beta'}). \quad (6.19b)$$

and $M_m^{S_d}(\lambda_a\lambda_\beta)$ is defined by Eq. (6.2). The explicit expression of the distribution function $W(\theta_c\varphi_c; \theta_d\varphi_d)$ will be found in Ref. 84 for the processes $K^+p \rightarrow K^*N^*$ and $p\bar{p} \rightarrow N^*\bar{N}^*$. Parity conservation reduces the distribution function to the form

$$W(\theta_c\varphi_c; \theta_d\varphi_d) = \sum_{\substack{mm' \\ nn'}} R_e[M_{mm'}^{S_d}(\theta_d\varphi_d)M_{nn'}^{S_c}(\theta_c\varphi_c)]R_e[\rho_{nn'}^{mm'}], \quad (6.20)$$

hence, also in this case we can learn only the real parts of the joint density matrix.

6. 2 Regge pole analysis and possible modifications

In this subsection we are to describe to what extent the analyses have been made on the structure of the density matrix on the basis of the Regge pole model and to investigate the possible modifications. Without entering into details the Regge pole model makes some definite predictions about the density matrix.

(a) If only one Regge pole can contribute to the process, the density matrix is almost independent of incident energy. Example is the reaction (3) in Table VI.

(b) In the production of a resonant state of natural (unnatural) parity from an incident pseudoscalar meson, the density matrix element ρ_{00} is exactly zero if all the exchanged Regge poles have natural (unnatural) parities. Examples are the reactions (5) and (9) in Table VI.

Now the experimental data on the density matrices for various production processes are accumulating and it seems desired to analyze in detail the density matrix in order to test the Regge pole model and in practice the analyses are now in progress. In Table VI the results obtained so far are summarized. Some comments on this Table are in order.

(1) $\pi^-p \rightarrow \pi^0N^{*++}$

It has been pointed out^{57), 85), 86)} that this process is very useful to test the Regge pole model, since only ρ can be exchanged in the t -channel. Several authors attempted to describe this process by the ρ Regge pole exchange. In particular, Krammer and Maor⁵⁷⁾ used the correct residues (which are slowly varying functions of t) with kinematical factors factored out and found good agreement with experiment; energy-independent density matrix is consistent with the limited data available and the dip observed around $t \approx -0.6 \text{ GeV}/c$ is due to the wrong-signature nonsense zero in the ρ Regge amplitude. The available data are only at 4 and 8 GeV/c and more detailed data about the energy dependence of density matrix are desired.

(2) $\pi^+n \rightarrow \omega p, \pi^+p \rightarrow \omega N^{*++}$

If the ρ Regge pole exchange dominated these reactions, we would have a dip around $t \approx -0.6 \text{ GeV}/c$ and $\rho_{00} = 0$, both in contradiction to experiment. Experimentally, the angular distribution has a rather flat slope and $\rho_{00} \approx 0.5$ at 3 GeV/c⁵⁸⁾ and $\rho_{00} = 0.26 \pm 0.10$ at 8 GeV/c for the reaction $\pi^+p \rightarrow \omega N^{*++54)}$. (See Fig. 9)

The ρ -dip can be filled by a strong contribution of B meson (assuming $J^{PG} = 1^{++}$) which, at the same time, gives finite ρ_{00} ⁵⁹⁾.

Table VI.

	process	t -channel particle	experiment (p_L)(GeV/c)	Ref. (Theory)	
				Regge pole fit	OPE+ab-sorption fit
1	$\pi^+p \rightarrow \rho^+p$	$\pi A_1 A_2 \omega$	1.6, 2.7, 5, 4.0, 8.0. $\rho_{00}=0.5\sim 0.8$; $Re\rho_{10}=-0.074\sim -0.08$	(57)	(90)
2	$\pi^+n \rightarrow f^0p$	$\pi A_1 A_2$	4.0, 6.0, 10.0. $\rho_{00}\approx 1$	(57)	
3	$\pi^+p \rightarrow \pi^0 N^{*++}$	ρ	4.0, 8.0. $\rho_{33}=0.2\sim 0.4$ $Re\rho_{31}=0\pm 0.5$; $Re\rho_{3-1}=0\sim 0.2$	(57)(85) (86)	
4	$\rightarrow \rho^0 N^{*++}$	$\pi A_1 A_2$	2.77, 3.65, 4.0, 8.0. $\langle \rho_{00} \rangle = 0.74$; $\langle \rho_{1-1} \rangle \sim -0.003$		(90)
5	$\rightarrow \omega N^{*++}$	$\rho(B)$	8.0 $\rho_{00}\approx 0.26$; at lower energies $\rho_{00}\approx 0.5$.		
6	$\pi^-p \rightarrow f^0n$	$A_1 A_2 \pi$	as for $\pi^+n \rightarrow f^0p$	(57)	(90)
7	$\rightarrow \rho^-p$	$\pi A_1 A_2 \omega$	as for $\pi^+p \rightarrow \rho^+p$	(57)(87)	(90)
8	$\rightarrow \rho^0n$	$A_1 A_2 \pi$	4.0, 6.0, 8.0.	(57)(88)	(90)
9	$\pi^+n \rightarrow \omega p$	$\rho(B)$	1.7, 3.25. $ \rho_{00} > 0.5$ $\rho_{00}=0.60$; $\rho_{1-1}=0.0$; $Re\rho_{10}=-0.06$ at 1.7 GeV/c.	(59)	(90)
10	$K^+p \rightarrow K^0 N^{*++}$	$\rho A_1 A_2$	1.96, 3.0, 3.5, 5.0 $\langle \rho_{32} \rangle \sim 0.2$; $\langle Re\rho_{3-1} \rangle \sim 0$ at 3 GeV/c	(57)	(90)
11	$\rightarrow K^{*+}P$	$\pi \omega \varphi \dots$	3.0, 5.0 $\rho_{00}\sim 0.2$; $\rho_{1-1}=0.2\sim 0.4$; $Re\rho_{10}\sim 0$		
12	$\rightarrow K^*N^*$	$\pi \dots$	1.95, 3.0		(90)
13	$K^-p \rightarrow K^{*-}p$	$\rho \omega \varphi \dots$	3.0		(90)
14	$K^+n \rightarrow K^{*+}p$	$\pi \dots$	2.3		(90)
15	$K^-p \rightarrow \pi^- Y^*$	K^*	2.24 $\rho_{33}\sim 0.3$; $Re\rho_{3-1}\sim 0.27$; $Re\rho_{31}\sim 0.05$		(90)

(3) $\pi^\pm p \rightarrow \rho^\pm p$, $\pi^- p \rightarrow \rho^0 n$

For these reactions, experiments are made for larger energy region and rather accurate data are obtained. (For example, see Fig. 9.) Several authors analyzed these processes and get satisfactory results for the differential cross section and density matrix for $\pi^\pm p \rightarrow \rho^\pm p$ process with appropriate combination of π , A_1 (unnatural parity) and ω , A_2 (natural parity^{57), (57)}). However, for $\pi^- p \rightarrow \rho^0 n$ process where A_1 , A_2 is exchanged in the t -channel, Ringland and Thews⁵⁸⁾ obtained an upper bound for the parameter $|Re\rho_{10}|$ in the framework of Regge pole model and the value is clearly violated by experiment at 6 and 8 GeV/c.

Finally we comment about the non-Regge effects. In analogy to the discussion in § 5, some other contributions can be taken into account, i. e. the contribu-

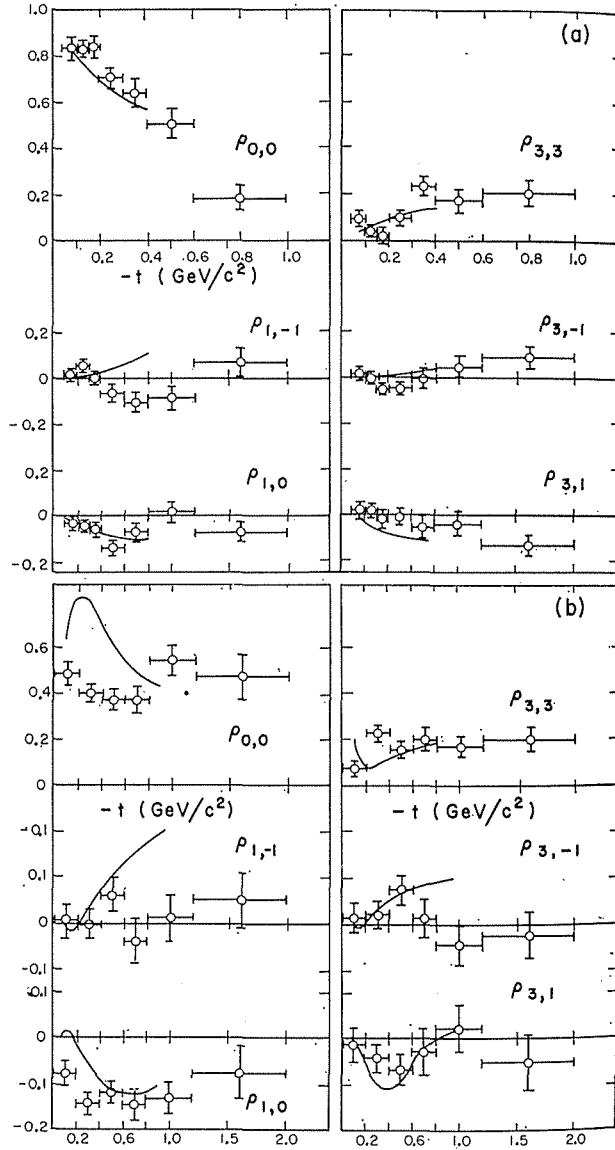


Fig. 9. Momentum transfer distributions of the density matrix elements for (a) $\pi^+p \rightarrow \rho^0 N^{*++}$ and (b) $\pi^+p \rightarrow \omega^0 N^{*++}$ between 3 and 4 GeV/c, measured by Brown et al. (Ref. 55). The solid lines are the predictions of the one-pion-exchange model with absorption, calculated at 4 GeV/c in Ref. 90.

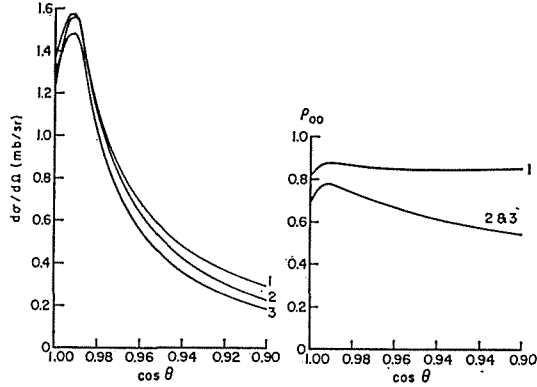


Fig. 10. The typical predictions of the one-pion-exchange model with absorption on the differential cross section and the density matrix element ρ_{00} for the reaction $\pi^- p \rightarrow \rho^- p$ at 4 GeV/c, calculated in Ref. 90. The coupling constants are $g^2_{\rho\pi\pi}/4\pi=2$, $g^2_{\pi N}/4\pi=14.0$ throughout. The absorption parameters for the initial state are $C_+=0.76$, $A_+=0.040$ throughout. These for the final state are, curve 1: $C_-=C_+$, $A_-=A_+$; curve 2: $C_-=1.00$, $A_-=A_+$; curve 3: $C_-=1.00$, $A_-=0.75 A_+$. Here the absorption parameters are defined by

$$e^{2i\delta_j(\pm)} \cong 1 - c_{\pm} e^{-A_{\pm} \left(j \pm \frac{1}{2}\right)^2}$$

with

$$c_{\pm} = \frac{\sigma_T^{(\pm)}}{4\pi\gamma_{\pm}}$$

and

$$A_{\pm} = \frac{1}{2k} \frac{1}{\gamma_{\pm}}$$

where $\delta_j^{(-)}$ and $\delta_j^{(+)}$ are the complex elastic scattering phase shifts in the final and initial channels, respectively, γ_{\pm} the parameters which appear in the elastic angular distribution (see Eq. (2.7) in sec. 2) and k the c. m. system momentum.

tions of s channel resonances, cuts in J plane, or absorptive corrections. The analyses are now in progress.⁸⁹⁾

It is convenient to show in Fig. 10 the typical effect of absorptive correction in OPE model,⁹⁰⁾ from which we see the absorptive correction changes appreciably the spin density matrix while it does not lead to significant changes in the differential cross sections.

§ 7. Concluding remarks

In the preceding sections we have presented a systematic and critical review of the phenomenological Regge pole theory, and in this final section we attempt first to summarize the complicated situation and second to remark some new aspects of the Regge pole approach to high energy scatterings.

(1) It has been widespread speculation that the Pomernanchuk trajectory has a quite small slope (say, $1/3$ (GeV/c)⁻²) and does not correspond to any observed particles; it serves only as a good tool in fitting to cross section data.

Our feeling is that the Pomeranchuk pole is simply a realization in the complex angular momentum plane of shadow scattering which plays a dominant role in the high energy region but all the effects of shadow or inelastic scatterings may not be represented in terms of only the singularities in the complex J -plane. From phenomenological point of view one can construct a model based on the Regge pole hypothesis without the Pomeranchon; instead of the P one simply takes a shadow model.⁷⁸⁾ This combination of the Regge pole and shadow models also seems to tend to eliminate some of difficulties in the pure Regge pole model.

(2) Let us mention the various dip mechanisms.⁹¹⁾ On the one hand, the old dip mechanism of sense choosing at the nonsense values of the wrong signature proves to be valid only if the effects of the third double spectral function are neglected; if otherwise and as long as the effects are small, the position of the dip will be shifted slightly from the point where one would have one according to the old dip mechanisms, as argued by Mandelstam and Wang.⁴¹⁾ On the other hand, one cannot say too much about which of the various mechanisms trajectories of even signature obey at $J=0$; sense choosing, nonsense choosing, Chew's⁵⁾, Gell-Mann's⁶⁾ and non-compensation mechanisms⁶³⁾. A dynamical model for a trajectory would be necessary to attack this problem from the theoretical point of view.

(3) A parity-doubled conspiracy (Gribov phenomenon⁷⁾) of Fermion Regge pole is to be tested experimentally by measuring the polarization parameters for meson-nucleon scattering in the backward hemisphere. Dips in angular distributions of backward π^+p and K^+p scatterings are of special interest; do they really originate from the signature zeros? If so, why do the exchange force take a special role at a particular value of four momentum transfer? We have to pursue the dynamical origin of the signature zeros.

(4) We mention an interesting question of evasions versus conspiracies which belongs to the subject of the second paper. Kinematical constraints on forward helicity amplitudes (which we call conspiracy relations) can be satisfied either by vanishing residues (evasions) or by correlation in position and residue of the relevant Regge poles (conspiracies). Only the latter possibility allows the double helicity flip amplitudes which conserve angular momentum in the forward direction to contribute with full strength. Thus Regge trajectories of unnatural parity $P=(-1)^{J+1}$ can contribute through conspiracies to forward NN and $\bar{N}N$ scatterings⁹²⁾ at high energies or to forward production processes $A+N \rightarrow B+N$. It may be interesting to speculate that the (sharp) forward peaks of the reactions $p n \rightarrow n p$, $\bar{p} p \rightarrow \bar{n} n$ ⁹²⁾ and $\bar{p} p \rightarrow \bar{A} A$ ⁹³⁾ are due to conspirators of π and K Regge poles. Forward productions of vector mesons are also of importance since conspiracies of classes II and III in the terminology of Freedman and Wang⁹⁾ may coexist.⁹⁴⁾

(5) Polarization test is useful to refine the Regge model at a deeper level. More accurate energy variation of $P(\theta)$ for the reaction $\pi^-p \rightarrow \pi^0 n$ is necessary to distinguish the various models discussed in § 5.3. It is also helpful to detect presence or absence of polarization in $\pi^-p \rightarrow \eta n$ in order to test the single R pole model. If finite polarization results, we may add the conspirator of π (with the same conventional quantum numbers as the A_2) to the R contribution. It will be interesting to speculate at this stage that small imaginary parts of

trajectory and residue functions would not violate Mandelstam analyticity under certain circumstances, as suggested by Chen and Sharp⁹⁵⁾; in such a case we may have finite polarization. Reeder and Sarma³⁸⁾ calculated the polarization parameters for $K^-p \rightarrow \bar{K}^0n$ which have to be checked experimentally. $P(\theta)$ for nucleon charge exchange scatterings would provide a critical test of the Phillips conspirator model.⁹⁶⁾ Detection of presence or absence of energy dependence of $P(\theta)$ for $\pi^\pm p \rightarrow \pi^\pm p$ with more accuracy is also of importance.

(6) Application of the Regge pole model to certain production processes for small momentum transfers has been made with particular emphasis on the decay correlation. Until now data on density matrix are not sufficient and contain rather large errors so that definite conclusion of the applicability cannot be drawn. It should be remembered that the one-particle exchange model with absorption can explain decay angular correlation with remarkable success.⁹⁰⁾

Finally, we describe some new proposals recently made in connection with the Regge pole theory.

An interesting fact was pointed out by Tanaka et al.⁹⁷⁾ that the Regge pole behaviour may be closely related to the propagation of an extended particle. They investigated Yukawa's bi-local field as a simple example and reached the following conclusions. "The extended particle quantized so as to represent Regge pole behaviour behaves almost equivalently to the superposition of local fields with different intrinsic spins when it propagates with a time-like four momentum, but it quite differently behaves when it propagates with a space-like four momentum." This indicates that the exchange of one Reggeon can never be equivalent to the exchange of a series of elementary particles with different intrinsic spins, so far as it has a space-like four momentum,⁹⁸⁾ in contradiction to the discussions recently made by Van Hove.⁹⁹⁾ According to the statement of Van Hove, "the exchange of an infinite series of particles with the mass formula of Regge type is equivalent to the exchange of Regge trajectory itself." He did not make clear distinction whether the particle has a space-like or time-like four momentum.¹⁰⁰⁾

Anyway, several authors have recently investigated the Regge pole model in relation to his discussion, one of which is that of Halpern.¹⁰¹⁾ According to his discussion, "all the particles but perhaps the lowest member in the series must be composite in order to introduce consistently with unitarity in the s channel", which is very interesting though only from a view-point of bootstrap mechanism for the composite particle. At the same time, we must notice several attempts recently made about the internal relativistic spin angular momentum from the group theoretical point of view.^{91,102)} On the other hand, an attempt is being made to understand the characteristic features of Regge pole model from a standpoint of composite model. As a first step, Yoshida and Machida¹⁰³⁾ take the ρ trajectory which is assumed to be composed of a quark and an antiquark. They calculated the trajectory and residue function assuming a simple potential between a quark and an antiquark, and obtained results consistent with the experiment.

Thus the situation seems to tend one to regard the Regge behaviour as being due to the propagation of particle with internal structure. Then the scattering amplitude should naturally include absorption correction in addition

to the Regge pole exchange contribution, which will change such quantities as polarization parameters or density matrices.

We would like to expect that systematic analysis of the high energy reactions by the Regge pole model may be one of the important means to shed light on the structure of hadrons.

ACKNOWLEDGEMENTS

This work was prepared for the research meeting for high energy physics held at The Research Institute for Fundamental Physics, September in 1967. The authors would like to thank Professor S. Machida and other members of the meeting. Thanks are also due to Miss E. Marumoto and Miss C. Nakamura for typing the manuscript.

REFERENCES AND FOOTNOTES

- 1) S. C. Frautschi, "Regge Poles and S-Matrix Theory", W. A. Benjamin, Inc., New York, 1963; R. G. Newton, "The Complex j -Plane", W. A. Benjamin, Inc., New York, 1963; E. J. Squires, "Complex Angular Momenta", W. A. Benjamin, Inc., New York, 1963.
- 2) W. G. Wagner and D. H. Sharp, *Phys. Rev.* **128**, 2899 (1962).
- 3) A. Ahmadzadeh and E. Leader, *Phys. Rev.* **134**, B1058 (1964).
- 4) M. Gell-Mann, Proceedings of the International Conference on High Energy Physics, Geneva, p. 533, 1962.
- 5) G. F. Chew, *Phys. Rev. Letters* **16**, 60 (1966).
- 6) C. B. Chiu and J. D. Stack, *Phys. Rev.* **153**, 1575 (1967).
- 7) V. N. Gribov, *Soviet Phys. -JETP* **16**, 1080 (1963).
- 8) D. V. Volkov and V. N. Gribov, *Soviet Phys. -JETP* **17**, 720 (1963).
- 9) D. Z. Freedman and J. M. Wang, *Phys. Rev.* **153**, 1596 (1967); *ibid.* **160**, 1560 (1967).
- 10) L. Durand, III, *Phys. Rev. Letters* **18**, 58 (1967).
- 11) V. Singh, *Phys. Rev.* **129**, 1889 (1963).
- 12) H. Lohrman et al., *Phys. Letters* **13**, 78 (1964).
A. E. Taylor et al., *Phys. Letters* **14**, 54 (1964).
K. J. Foley et al., *Phys. Letters* **14**, 74 (1964).
G. Bellettini et al., *Phys. Letters* **14**, 164 (1964); *ibid.* **19**, 705 (1965).
L. Kirillova et al., *Phys. Letters* **13**, 93 (1964); *Sov. Jour. Nucl. Phys.* **1**, 379 (1965).
G. Baroni et al., *Nuovo Cim.* **38**, 95 (1965).
- 13) G. Bellettini et al., *Phys. Letters* **19**, 341 (1965).
Kh. Chervnev et al., "Small-Angle Proton-Deuteron Elastic Scattering at the Energy 1 to 10 GeV/c", quoted by L. Van Hove in Proceedings of the XIIIth International Conference on High-Energy Physics, University of California Press, Berkeley, 1967 (hereafter referred to as B).
L. Kirillova et al., "Small Angle p-d Elastic Scattering at the Energies 1 to 10 GeV/c", quoted by L. Van Hove in B.
- 14) K. J. Foley et al., *Phys. Rev. Letters* **14**, 862 (1965); *ibid.* **19**, 193 (1967).
- 15) W. de Baere et al., *Nuovo Cim.* **45A**, 885 (1966).
- 16) J. Mott et al., *Phys. Letters* **23**, 171 (1966).
- 17) K. J. Foley et al., *Phys. Rev. Letters* **11**, 425 and 503 (1963); *ibid.* **15**, 45 (1965).
- 18) M. N. Kreisler et al., *Phys. Rev. Letters* **16**, 1117 (1966).
- 19) I. Mannelli et al., *Phys. Rev. Letters* **14**, 408 (1965).
A. V. Stirling et al., *Phys. Rev. Letters* **14**, 763 (1965).
P. Sonderegger et al., *Phys. Letters* **20**, 75 (1966).

- 20) O. Guisan et al., Phys. Letters 18, 200 (1965).
- 21) P. Astbury et al., Phys. Letters 16, 329 (1965); *ibid.* 23, 396 (1966).
- 22) H. Palevsky et al., Phys. Rev. Letters 9, 509 (1962).
J. L. Friedes et al., Phys. Rev. Letters 15, 38 (1965).
G. Manning et al., Nuovo Cim. 41, 167 (1966).
- 23) R. Armenteros et al., Phys. Rev. 119, 2068 (1960).
C. K. Hinrichs et al., Phys. Rev. 127, 617 (1962).
O. Czyzewski et al., Phys. Letters 20, 554 (1966).
P. Astbury et al., Phys. Letters 22, 537 (1966).
- 24) C. Baltay et al., Phys. Rev. 140, B1027 (1965).
C. Y. Chien et al., Phys. Rev. 152, 1171 (1966).
- 25) G. Smith et al., Phys. Rev. 123, 2160 (1961).
A. R. Clyde, "Proton-Proton Elastic Scattering at Incident Momenta 3, 5, and 7 GeV/c", reported by A. Whetherell in B.
- 26) B. Barish et al., Phys. Rev. Letters 17, 720 (1966).
- 27) W. M. Katz et al., Phys. Rev. Letters 19, 265 (1967).
- 28) C. T. Coffin et al., Phys. Rev. Letters 15, 838 (1965).
C. T. Coffin et al., " π^+p Elastic Differential Cross Sections from 2.3 to 4.0 GeV/c", quoted by L. Van Hove in B.
- 29) J. Orear et al., Phys. Rev. 153, 1162 (1966).
- 30) S. W. Kormanyos et al., Phys. Rev. Letters 16, 709 (1966).
H. Brody et al., Phys. Rev. Letters 16, 828 and 968 (1966).
W. R. Frisken et al., Phys. Rev. Letters 15, 313 (1965).
- 31) A. Ashmore et al., Phys. Rev. Letters 19, 460 (1967).
- 32) J. Banaigs et al., Phys. Letters 24B, 317 (1967).
- 33) Regge pole formalism for scattering of spinning particles has been presented by several authors. See, for instance, A. H. Mueller and T. L. Trueman, Phys. Rev. 160, 1296 (1967) in which the past references were listed.
- 34) R. K. Logan, Phys. Rev. Letters 14, 414 (1965).
- 35) R. Phillips and W. Rarita, Phys. Rev. 139, B1336 (1965).
- 36) F. Arbab and C. Chiu, Phys. Rev. 147, 1045 (1966).
- 37) S. C. Frautschi, Phys. Rev. Letters 17, 721 (1966).
- 38) D. Reeder and K. V. L. Sarma, reported by V. Barger at the Symposium on Regge Poles, Argonne National Laboratory, 1967. See also Nuovo Cim. 51A, 169 (1967).
- 39) P. Bonamy et al., Phys. Letters 23, 501 (1966).
- 40) This is the only unsatisfactory aspect of the ρ pole dominance model of the reaction $\pi^-p \rightarrow \pi^0n$. Since polarization depends sensitively on small secondary effects like resonance formation in the direct channel or the exchange of other singularities in the complex J -plane, the single- ρ -pole description of the π^-p charge exchange reaction may remain approximately valid, even if the finite polarization result persists at higher energies. See Sec. 5.
- 41) When a trajectory $\alpha(t)$ with signature P_J goes through an integral value J_0 , it is said that, if $(-1)^{J_0} = +P_J(-P_J)$, J_0 is right (wrong) signature of the trajectory. Furthermore, when $J_0 \geq \Delta\lambda (< \Delta\lambda)$ with $\Delta\lambda$ the magnitude of the helicity flip in some channel to which the trajectory couples, we refer to the channel as sense (nonsense). For theories with a third double spectral function Mandelstam showed that the Froissart-Gribov continuation has generally fixed singularities at the nonsense values of wrong signature. If such is the case for the ρ amplitude, the dip mechanism discussed in the text lose any significant meaning (note that $\alpha_\rho(t) = 0$ is the nonsense value of wrong signature of the ρ trajectory). See, for instance, Ref. 33) and S. Mandelstam and L.-L. Wang, Phys. Rev. 160, 1490 (1967).
- 42) R. J. N. Phillips and W. Rarita, Phys. Rev. Letters 15, 807 (1965).
- 43) R. J. N. Phillips and W. Rarita, Phys. Letters 19, 598 (1965).
- 44) R. J. N. Phillips and W. Rarita, Phys. Rev. 140, B200 (1965).

- 45) R. J. N. Phillips, Nucl. Phys. **B1**, 572 (1967).
- 46) K. A. Ter-Martirosyan, reported by L. Van. Hove in B.
- 47) Here we visualize the form of the R trajectory similar to that of the ρ . If the slope of the R trajectory is quite small for negative t , the above arguments fail to be applied for distinguishing the two mechanisms. Unfortunately, the available data on various charge exchange scatterings cannot resolve such ambiguities (F. Arbab, N. F. Bali, and J. W. Dash, Phys. Rev. **158**, 1515 (1967)).
- 48) L. L. Wang, Phys. Rev. **153**, 1664 (1967).
- 49) Saclay-Orsay-Bari-Bologna Collaboration, Phys. Letters **13**, 341 (1964).
- 50) M. Abolins et al., Phys. Rev. **136**, B195 (1964).
- 51) German-British Collaboration, Phys. Letters **10**, 229 (1964).
- 52) German-British Collaboration, Nuovo Cim. **34**, 495 (1964); Phys. Rev. **138**, B897 (1965).
- 53) Aschen-Berlin-CERN Collaboration, Phys. Letters **19**, 608 (1965).
- 54) Aachen-Berlin-CERN collaboration, Phys. Letters **22**, 533 (1966).
- 55) D. Brown et al., Phys. Rev. Letters **19**, 664 (1967).
- 56) H. O. Cohn et al., Phys. Letters **15**, 344 (1965).
- 57) R. L. Thews, Phys. Rev. **155**, 1624 (1967).
M. Krammer and U. Maor, Nuovo Cim. **50A**, 963 (1967).
- 58) A. H. Rosenfeld et al., Rev. Mod. Phys. **39**, 1 (1967).
- 59) M. Barmawi, Phys. Rev. Letters **16**, 595 (1966).
- 60) W. Galbraith et al., Phys. Rev. **138**, B913 (1965).
- 61) Since the R trajectory has even signature, $\alpha_R(t)=0$ is nonsense value of right signature. See foot-notes 41) and 47).
- 62) See p. 270 of B.
- 63) Recently new dip mechanism has been proposed by C. B. Chiu, S. Y. Chiu and L.-L. Wang (Phys. Rev. **161**, 1563 (1967)). According to them, the P' trajectory chooses the non-compensation mechanism in such a way that the helicity non-flip amplitude of the P' trajectory vanishes at $\alpha_{P'}=0$. The P trajectory does not cross spin zero. They then propose that the secondary minima in the low-energy $\pi^\pm p$ and $\bar{p}p$ elastic scatterings are due to the vanishing of the helicity nonflip P' amplitude. We argue that, although the P' and the R trajectories seem to belong to the same tensor nonet, the latter cannot enjoy the same mechanism since we have no dip in $\pi^-p \rightarrow \eta n$. On the other hand, using the finite energy sum rules which connect the Regge pole parameters controlling the high energy amplitude with the low energy integrals involving resonance parameters, several authors have tried to eliminate phenomenological ambiguities in the Regge pole model. See, for instance, R. Dolen, D. Horn, and C. Schmid, Phys. Rev. Letters **19**, 402 (1967) and S. Matsuda and K. Igi, *ibid.*, **19**, 928 (1967).
- 64) V. Flores-Maldonads, Phys. Rev. **155**, 1773 (1967).
- 65) S. Mandelstam, Ann. Phys. **19**, 254 (1962).
- 66) The fact that Fermion trajectory has left cut implies that, even if only one Fermion pole is exchanged, spin-flip and -nonflip amplitudes have different phases leading to finite polarization. See J. D. Stack, Phys. Rev. Letters **16**, 286 (1966).
- 67) Relations between $f_{1,2}$ of Eq. (4.3) and f, g , of Eq. (5.1) in Sec. 5 are

$$f(\sqrt{s}, u) = f_1(\sqrt{s}, u) - \cos\theta f_1(-\sqrt{s}, u),$$

$$g(\sqrt{s}, u) = -\sin\theta f_1(-\sqrt{s}, u),$$

with

$$f_2(\sqrt{s}, u) = -f_1(-\sqrt{s}, u).$$

In Eq. (4.4),

$$E_s = \frac{s + M^2 - m_\pi^2}{2\sqrt{s}}, \quad E_u = \frac{u + M^2 - m_\pi^2}{2\sqrt{u}},$$

M = nucleon mass.

- 68) V. Barger and D. Cline, Phys. Rev. Letters 16, 913 (1966); Phys. Rev. 155, 1792 (1967).
- 69) In this subsection, we follow the work of D. Cline, C. Moore, and D. Reeder, Phys. Rev. Letters 19, 675 (1957).
- 70) M. Borghini et al., Phys. Letters 24B, 77 (1966).
- 71) C. B. Chiu, R. Phillips, and W. Rarita, Phys. Rev. 153, 1485 (1967).
- 72) R. K. Logan, J. Beaupre and L. Sertorio, Phys. Rev. Letters 18, 258 (1967).
- 73) H. Hogaasen and W. Fisher, Phys. Letters 22, 516 (1966). See also H. Hogaasen and A. Frisk, Phys. Letters 22, 90 (1966).
- 74) There is the independent support for the introduction of the ρ' . Sources are: 1) The isovector electromagnetic form factor of the nucleon (C. H. Chan et al., Phys. Rev. 141, 1298 (1966) and E. B. Hughes et al., Phys. Rev. 139, 3458 (1965)), 2) SU (3) \times SU (3) symmetry analysis (S. K. Bose, Nuovo Cim. 46A, 419 (1966) and 3) the missing-mass spectrometer experiment (W. Kienzle, Phys. Letters 19, 438 (1965) and D. D. Allen et al., Phys. Letters 22, 543 (1966)). If we identify the $\delta(963 \pm 5$ with $I < 1$) observed by Kienzle et al. as the ρ' and further assume that the ρ' trajectory has a linear t dependence with the same slope as the ρ , we have
- $$\alpha_{\rho'}(t) = 0.17 + 0.9t$$
- which was used in Ref. 72).
- 75) R. K. Logan and L. Sertorio, Phys. Rev. Letters 17, 834 (1966).
- 76) V. M. de Lany et al., Phys. Rev. Letters 18, 149 (1967).
- 77) S. Mandelstam, Nuovo Cim. 30, 1148 (1963).
- 78) G. Cohen et al., Nuovo Cim. 48, 1075 (1967).
- 79) See, for instance, R. C. Arnold, Phys. Rev. 140, B1022 (1965).
- 80) A. Bialas and L. Van Hove, Nuovo Cim. 38, 1385 (1965).
- 81) K. Gottfried and J. D. Jackson, Nuovo Cim. 33, 309 (1964); Nuovo Cim. 34, 735 (1964).
- 82) M. Jacob and G. C. Wick, Ann. Phys. 7, 404 (1959).
- 83) T. L. Truemen and G. C. Wick, Ann. Phys. 26, 322 (1964).
- 84) H. Pilkuhn and B. E. Y. Svensson, Nuovo Cim. 38, 519 (1965).
- 85) A. Iwaki, to be published in Prog. Theor. Phys.
- 86) See p. 271 of B.
- 87) M. L. Paciello and A. Pugliese, Phys. Letters 24B, 431 (1967).
- 88) G. A. Ringland and R. L. Thews, preprint. "Bound for effective polarization in ρ production in a Regge-pole exchange model".
- 89) K. Koike and M. Nobuyama, private communication.
- 90) J. D. Jackson, J. T. Donohue, K. Gottfried, R. Keyser and E. E. Y. Svensson, Phys. Rev. 139, B428 (1965).
- 91) W. Drechsler, "Fixed Singularities in The Angular Momentum Plane and Dip Mechanisms", CERN preprint, 1967.
- 92) R. J. N. Phillips, Nucl. Phys. B2, 394 (1967).
- 93) K. Morita, Prog. Theor. Phys. 39, 531 (1968); Erratum, 40, 192 (1968).
- 94) R. F. Sawyer, Phys. Rev. Letters 18, 1212 (1967); *ibid.* 19, 137 (1967).
S. Frautschi and L. Jones, "Conspiracy Relations in Vector Meson Production", to be published in Phys. Rev. H. Hogaasen and Ph. Salin, Nucl. Phys. B2, 657 (1967) L. Bertocchi, "Conspiracies and Forward Production of Vector Mesons", CERN preprint, TH. 842, 1967.
- 95) H. Cheng and D. Sharp, Ann. Phys. 22, 481 (1963).
- 96) S. Machida, private communication.
- 97) M. Bando, T. Inoue, Y. Takada, and S. Tanaka, Prog. Theor. Phys. 38, 715 (1967).
T. Shirafuji, Prog. Theor. Phys. 39, 1047 (1968).
- 98) This may be convinced from the condition of validity of the Legendre expansion;

$$\frac{P_\alpha(-z)}{\sin\pi\alpha} = \frac{1}{\pi} \sum_{l=0}^{\infty} \left[\frac{1}{\alpha-l} - \frac{1}{\alpha+l+1} \right] P_l(z)$$

when $|z| < 1$.

- 99) L. Van Hove, Phys. Letters **24B**, 183 (1967).
- 100) S. Tanaka, Soryusiron Kenkyu, Mimeographed Circular in Japanese, **35**, 395 (1967).
- 101) M. B. Halpern, Phys. Rev. **159**, 1328 (1967).
- 102) M. Toller, Nuovo Cim. **53A**, 671 (1968).
- 103) T. Yoshida and S. Machida, Prog. Theor. Phys. **39**, 1304 (1968).